AALBORG UNIVERSITET

Enhanced photosynthesis and characterisation of carbohydrate production of *Synechococcus* PCC 7002

By

David Sánchez Romero and Christine Sophie Steffen

Supervised by

Dr. Yumiko Sakuragi, Dr. Cristiano Varrone and Dr. Mette Lübeck

In collaboration with

Department of Plant and Environmental Sciences of Copenhagen University

A thesis submitted to Aalborg University Department of Sustainable Biotechnology as part of the requirement of the MSc Sustainable Biotechnology

10th June 2019

Abstract

Cyanobacteria are promising producers of carbohydrates from CO_2 as feedstock in biorefineries due to the lack of requirement for arable land. To increase carbohydrate production, photosynthesis was enhanced in *Synechococcu*s PCC 7002 by overexpressing bifunctional fructose 1,6-bisphosphatase/sedoheptulose 1,7-bisphosphatase (BiBPase). Growth and carbohydrate composition of *Synechococcus* PCC 7002 wild type and trcBiBP mutant was studied and compared. Physiological differences were analysed with OD_{730} measurements, microscopies and Nile Red staining. Glucose, sucrose, glycogen and cellulose were quantified by enzymatic digestion and subsequent glucose quantification by colorimetric GOPOD assay. TrcBiBP showed increased cell size, slower growth, higher glycogen and cellulose content than wild type. However, the increase of carbohydrates was not statistically significant, likely due to variability in the growth conditions of the experimental setup. The results were partially inconsistent to a previous study in which trcBiBP showed faster growth and lower glycogen content than wild type (De Porcellinis et al., 2014). This contradiction was potentially caused by different methodologies regarding selection and maintenance of trcBiBP cells. The slower growth was hypothesized to be caused by insufficient nitrogen in the medium. However, nitrogen deprivation was found to barely affect growth and glycogen production of trcBiBP. In contrast, consistently with literature studies (Möllers et al., 2014) nitrogen deprivation lead to a significant increase of glycogen content in *Synechococcu*s PCC 7002 wild type, making it the more promising candidate to produce carbohydrates for biorefineries.

Table of contents

1 Introduction *1*

2 Materials and methods *2*

2.1 Native strain and constructed strain **2**

2.2 Transformation of *Synechococcus* 7002 **3**

2.3 Culture conditions **4**

2.4 Experiment 1: Growth and carbohydrate characterisation **5**

2.4.1 Characterization of growth 6

2.4.1.1 Cell density and morphology 6

2.4.1.2 Protein quantification 7

2.4.1.3 Nile red staining 7

2.4.2 Saccharides analysis 8

2.4.2.1 Processing for carbohydrate analysis 8

2.4.2.1.1 Separation of cell pellet and spent medium 8

2.4.2.1.2 Cell disruption 8

2.4.2.2 Analysis of glucose, sucrose, glycogen and cellulose 8

2.4.2.2.1 First approach: ethanol precipitations 8

2.4.2.2.2 Revision and testing of carbohydrates analysis method 10

2.4.2.2.3 Final approach of carbohydrates analysis 12

2.4.2.2.4 GOPOD assay 13

Measurements and calculations 13

Measurement and calculation of glucose 13

Measurement and calculation of sucrose, glycogen and cellulose 13

2.4.2.3 Analysis of total sugars 14

2.4.2.3.1 TFA hydrolysis and DNS assay 14

2.5 Experiment 2: Effect of position in aquarium tank on growth **14**

2.6 Experiment 3: Effect of initial $NaNO_3$ concentration on growth and glycogen content **15**

2.7 Statistical analysis **15**

3 Results *16*

3.1 Transformation of Synechococcus 7002 **16**

3.2 Experiment 1: Growth and saccharide characterization **16**

3.2.1 Cell size 16

3.2.2 Cell count per OD 18

3.2.3 Protein quantification 18

3.2.4 Nile red staining 19

3.3 Processing **20**

3.3.1 Cell disruption efficiency 20

3.4 Saccharide analysis **20**

3.4.1 Method testing 21

3.4.2 Carbohydrates analysis 21

3.4.3 Reliability of enzymatic carbohydrate digestion and GOPOD assay 25

3.5 Experiment 2: Effect of position in aquarium tank on growth **25**

3.6 Experiment 3: Effect of initial $NaNO_3$ concentration on growth and glycogen content **27**

4 Discussion ***29***

4.1 Growth characterisation and effect of nitrogen **29**

4.2 Saccharides analysis **31**

4.3 Evaluation of wild type or trcBiBP to produce feedstock for biorefineries **35**

5 Conclusions ***35***

6 Acknowledgements ***36***

7 Bibliography ***37***

8 Appendix ***40***

List of figures and tables

Figure 1: Scheme of *pDFtrc* vector. 3
Figure 2: Schematic tri-parental conjugation 3
Figure 3: Picture of aquarium tank setup 5
Figure 4: Schematic distribution of test tubes in aquarium tank in experiment 1. 6
Figure 5:Schematic outline of method 1 for carbohydrate digestion and analysis. 9
Figure 6: Schematic overview of testing three different methods 11
Figure 7: Schematic outline of method 3 for carbohydrate digestion and analysis.. 12
Figure 8: Gel electrophoresis of PCR amplified products using specific primers 16
Figure 9: Pictures of *Synechococcus 7002*. 17
Figure 10: OD_{730nm} measurements of the different biological replicates 17
Figure 11: Total protein content of the three genotypes 18
Figure 12: Pictures of *trcBiBP* stained with Nile red 19
Figure 13: Pictures of *trcBiBP* cells taken with confocal microscopy 20
Figure 14: Method testing 21
Figure 15: Intracellular carbohydrates analysis 22
Figure 16: Average intracellular glycogen and cellulose content per genotype 23
Figure 17: Total reducing sugars of each biological tripliacte estiamted with DNS 24
Figure 18: Reliability of enzymatic carbohydrate digestion and GOPOD assay 25
Figure 19: Effect of position in aquarium tank on growth. 26
Figure 20: Effect of initial $NaNO_3$ concentration on growth and protein content 28
Figure 21: Effect of initial $NaNO_3$ concentration glycogen 29

Table 1: Physiological characteristics of *wild type* and trangenic strains of *Synechococcus 7002* 18

List of abbreviations

ADP - adenosine diphosphate

ATP - adenosine triphosphate

BCA - bicinchoninic acid

BiBpase - bifunctional fructose 1,6- bisphosphatase/sedoheptulose 1,7-bisphosphatase

BSA - bovine serum albumin

DNA - deoxyribonucleic acid

DAPI - 4′,6-diamidino-2-phenylindole

DNS - 3,5-dinitrosalicylic acid

EV - empty vector

Fw - forward primer

FITC - fluorescein isothiocyanate

FBP- fructose-1,6-bisphosphate

F6P - fructose-6-phosphate

GO - glucose oxidase

G3P - glyceraldehyde-3-phosphate

HPLC - high-performance liquid chromatography

LB - lysogeny broth

NADPH - nicotinamide adenine dinucleotide phosphate hydrogen

N - standard nitrogen medium

N- - nitrogen depleted medium

N+ - nitrogen enriched medium

OD - optical density

PCC - pasteur culture collection

Rv - reverse primer

PBP- phycobilisomes

PCR - polymerase chain reaction

POD - peroxidase

SBP - sedoheptulose-1,7-bisphosphate

S7P - sedoheptulose-7-phosphate

TRITC - tetramethylrhodamine

TFA - trifluoroacetic acid

WT - wild type

1 Introduction

The use of petroleum-based fuels and materials has led to depletion of natural resources and a human-induced climate change (Höök & Tang, 2013). Therefore, there is need for sustainable alternatives to petroleum-based materials and fuels. A possible alternative to traditional oil refineries are biorefineries. Biorefineries integrate the conversion of biomass into products via chemical and biotechnological processes. They are capable of producing a variety of products such as fuels, chemicals and biomaterials from a biomass feedstock. The biomass feedstock consists mainly of carbohydrates, lignin, proteins and fats. For instance, glucose can be chemically or microbiologically converted to industrially relevant intermediates such as lactic acid, ethanol, acetic acid and levulinic acid (Kamm & Kamm, 2004). However, glucose from first generation biomass such as maize, rice or wheat crops compete with food resources due to the requirement of arable land and fresh water (Sánchez & Cardona, 2007). In contrast, marine cyanobacteria produce carbohydrates from CO_2 fixation without requiring arable land and requiring less fresh water. These carbohydrates can be used as feedstock in biorefineries.

For instance, the unicellular marine cyanobacterium *Synechococcus* PCC 7002 (hereafter *Synechococcus* 7002) has been successfully used as feedstock for yeast to produce bioethanol. After cultivation, *Synechococcus* 7002 cells were pelleted and enzymatically digested. The hydrolysates were used to grow *Saccharomyces cerevisiae* which fermented the present carbohydrates to ethanol (Möllers et al., 2014). *Synechococcus* 7002 is widely used for biotechnological applications due its fast growth (doubling time of 3-5 h) and tolerance of high salinity and high-light irradiation (Batterton and van Baalen, 1971). Physiological characteristics that along with its complete genome sequence (http://www.ncbi.nlm.nih.gov/nuccore/) and established genetic tools available (Markley et al., 2014) position it as a promising photosynthetic cell factory for metabolic engineering. Genetic modification can potentially further improve the promising physiological characteristics, making economic application more likely. De Porcellinis et al (2018) have enhanced photosynthesis in Synechococcus 7002 by overexpressing bifunctional fructose 1,6- bisphosphatase/sedoheptulose 1,7-bisphosphatase (BiBpase), a crucial enzyme in the Calvin-Benson-cycle.

In order to enhance the carbon uptake by photosynthetic CO_2 fixation, there is a need to improve and utilize the Calvin Benson cycle, responsible for C3 photosynthesis in cyanobacteria, as well as algae and most higher plants. Shortly, the cycle consists of a series of biochemical reactions, driven by NADPH and ATP molecules obtained by photosynthesis, to incorporate inorganic carbon from CO_2 into organic carbohydrates, namely glyceraldehyde-3-phosphate (G3P), and synthesize hexoses. This process involves several different enzymes and intermediates of three- to seven-carbon phosphorylated carbohydrates, which are also precursors for synthesis of a wide range of cellular building blocks. One of these enzymes, bifunctional fructose 1,6- bisphosphatase/sedoheptulose 1,7-bisphosphatase (BiBpase), is unique in cyanobacteria, since it catalyse the two separate dephosphorylations of fructose-1,6-bisphosphate (FBP) and sedoheptulose-1,7-bisphosphate (SBP) to fructose-6-phosphate (F6P) and sedoheptulose-7-phosphate (S7P) respectively. Reactions that in higher plants are taken over by two independent enzymes (Cotton et al., 2015).

Recently, the overexpression of BiBPase was found to cause a global reprogramming of the carbon metabolism in the cyanobacterium *Synechococcus* 7002 (De Porcellinis et al., 2018). This overexpression was conducted using the gene *slr2094*, BiBPase encoding gene of *Synechocystis*, in order to minimize the risk of homologous recombination. *Slr2094* gene was inserted in *pDFtrc* vector, which also contained a strong synthetic *trc* promoter and a spectinomycin resistance cassette. The transformation of *Synechococcus* 7002 with *pDFtrc* vector shown in Figure 1 was conducted by tri-parental conjugation and the resulting strain was designated *trcBiBP*.

The engineered strain showed a BiBPase activity 1.7 times higher than the *wild type* and many metabolic and physiological changes were found in *trcBiBP*. On the physiological aspect, *trcBiBP* showed a significantly increased cell length and area, whereas dry cell weight and cell count per OD_{730nm} were not altered from standard *wild type* values. Regarding the effects on the metabolism, immunodetection and proteomic analysis indicate that the overexpression enhanced the Calvin Benson cycle while repressing carbon catabolic pathways like the oxidative pentose phosphate pathway and glycolysis. Along with this, the quantification of glycogen and total sugars (intracellular and extracellular) showed lower glycogen content levels and a higher production of extracellular sugars compared to the *wild type*. To summarize, these observations by de Porcellinis et al. (2018), indicate that the overexpression of BiBPase in *Synechococcus* 7002 promotes carbon fixation and represses respiratory carbon metabolism, resulting in an increased photosynthetic growth and a redistribution of carbon towards non-storage carbohydrates.

The aim of the present study is to quantify and compare the carbohydrate composition of *Synechococcus* 7002 and the transgenic *trcBiBP*. The carbohydrates of interest are intracellular glycogen as main storage polysaccharide, intracellular cellulose as main polysaccharide present in the cell wall and intra- and extracellular glucose and sucrose. This research explores the effect of overexpressing the enzyme BiBPase on the carbohydrate metabolism of the cyanobacterium in order to evaluate its possible applications as feedstock for biorefineries such as bioethanol production from yeast.

2 Materials and methods

2.1 Native strain and constructed strain

The microorganism used for this project was *Synechococcus* 7002. Samples of *wild type Synechococcus* 7002 were obtained in cryo-tubes from the strain collection of the Department of Plant and Environmental Sciences of Copenhagen University. The content of those cryo-tubes was transferred to 50 ml petri dishes with solid A+ medium, which is defined further on and detailed in Appendix A. Several restreakings were conducted to obtain pure cultures due to contamination of the cryotubes.

Two strains were created through transformation of *Synechococcus* 7002 using the vector *pDFtrc* (Figure 1). The strains were denominated *trcBiBP and trcEV. TrcBiBP*, was transformed as described in de Porcellinis et al. (2018), in order to overexpress the enzyme BiBPase. *TrcEV* was transformed using a *pDFtrc* vector without a gene inserted in the multicloning site and therefore was denominated

"*EV*" from "*empty vector"*. This later strain was constructed as a negative control in order to detect metabolic alterations resultant only from the transformation process.

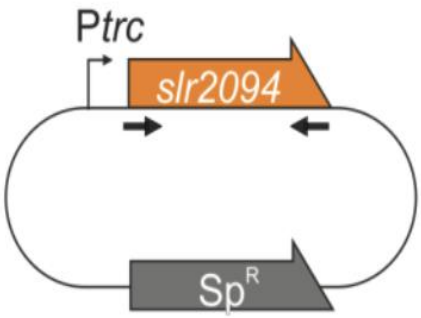

Figure 1: Scheme of pDFtrc vector. Plasmid used for transformation of Synechococcus 7002 containing trc promoter (Ptrc), spectinomycin resistance cassette (SpR) and slr2094 gene, BiBPase encoding gene from Synechocystis.

2.2 Transformation of *Synechococcus* 7002

Transformation was conducted by tri-parental conjugation (Figure 2) using the following *E. coli* cryo-stock strains: YS909 (*E. coli pRL443* conjugate strain, ampicillin resistant), YS910 (*E. coli pDF-trcBiBP* cargo strain, spectinomycin resistant) and YS724 (*E. coli pDF-trcEV* cargo strain, spectinomycin resistant).

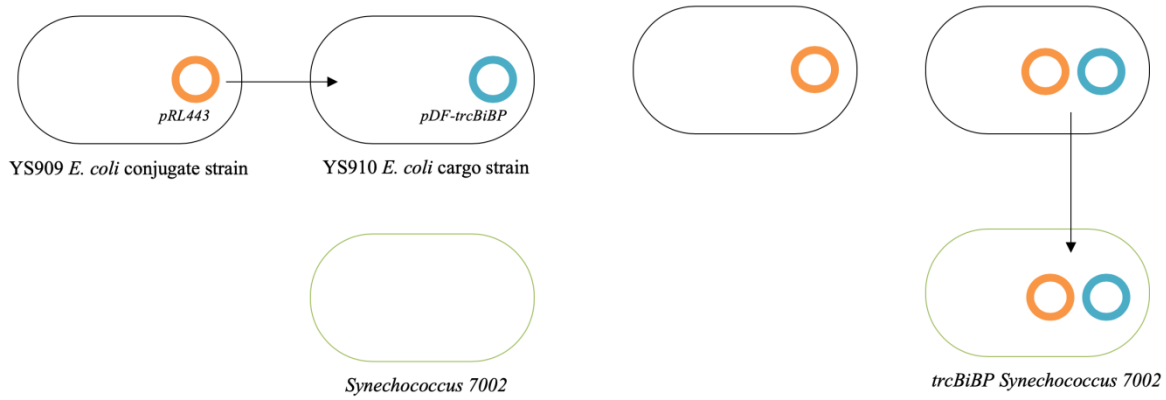

Figure 2: Schematic representation of tri-parental conjugation. Self-mobilizable conjugate plasmid pRL443 (orange) is transconjugated into the cargo strain (e.g. YS910). Cargo strain is now able to transconjugate the plasmid of interest (blue) into the recipient cell (green).

E. coli strains were resurrected by streaking on 50 ml petri dishes with solid LB medium supplemented with spectinomycin (50 µg/ml) or ampicillin (50 µg/ml) when appropriate. Plates were incubated at 37ºC upside down overnight. One colony from each genotype was transferred to 3 ml LB liquid medium with the respective antibiotic. Tubes were incubated at 37ºC and 220 rpm overnight. Simultaneously, *wild type Synechococcus* 7002 cells were cultured in test tubes with the same growth conditions as described in section 2.3.

After one day of incubation, *Synechococcus* 7002 cultures were centrifuged at 4000 rpm for 10 minutes, the supernatant was removed, and the pellet was resuspended in 5 ml A+ medium. OD_{730nm} was measured and the culture was diluted to a desired OD between 0.8 - 1. *E. coli* cultures were also

centrifuged in the same way and resuspended in 10 ml LB medium without antibiotics. Subsequently, 10 ml of each cargo strain (YS910 and YS724) were combined with 10 ml of conjugal strain (YS909) in 50 ml Falcon tubes. These two combinations were centrifuged once more to be resuspended in a final volume of 10 ml LB medium without antibiotics.

In Eppendorf tubes, 200 µl of each combined *E. coli* (cargo + conjugal strains) were mixed with 100 µl of *Synechococcus* 7002 in two different dilutions, 1:1 and 1:100. Mixtures were placed in the incubator at 25ºC and continuous light during 1 - 2 hours. After incubation, the mixtures were poured on A+ medium plates without antibiotics and dispersed among the plate by hand shaking. Plates were placed in the incubator at 25ºC and continuous light for 3 days. After 3 days, 500 µl of MiliQ water was added to the plates and cells were scraped with an inoculation loop and subsequently poured in plates supplemented with spectinomycin (50 µg/ml) in order to select for transformants. Two more plates with antibiotic were inoculated with *wild type* Synechococcus 7002 as a negative control. All plates were incubated at 37ºC under light for one week. The transformation was repeated due to observation of artefacts that are described in more detail in section 3.2.4.

Each biological replicate used in the growth and saccharide characterisation experiment was analysed with PCR and gel electrophoresis in order to confirm that the carbohydrate results corresponded to the right genotype. Cells were used as a template instead of purified plasmids. Samples were prepared by transferring 10 µl drops of the cultures to solid A+ medium with and without antibiotics. A few colonies were picked and diluted in MiliQ water and heated at 95ºC for 10 minutes. 1 µl from each diluted sample was transferred to PCR reaction mixture. *E. coli* strains YS909 and YS724 were used as positive controls. Samples and controls were placed in a thermocycler (Labcycler SensoQuest) to conduct the PCR reaction.

The presence of the transgene in *trcBiBP and trcEV* was tested by PCR amplification using the following target specific primers: 1Fw (5'- CCCGTTCTGGATAATGTT -3') and 1Rv (5' – GTTTCACTTCTGAGTTCG – 3'). These primers were specific for genotyping of the *pDFtrc* vector since they were complementary to the flanking regions of the multicloning site of this plasmid. The resultant product of the amplification using the plasmid containing BiBPase from *Synechocystis* has a size of 1353 bp, whereas the resultant product using the plasmid without BiBPase gene as a template has a size of 343 bp.

The resultant PCR products were separated by 1% agarose gel electrophoresis at 120 V for 45 minutes. Orange G dye was used to track DNA migration and 1 Kb plus DNA ladder was used to determine the size of the products.

2.3 Culture conditions

Synechococcus 7002 (*wild type, trcBiBP* and *trcEV*) cells were grown photoautotrophically in A+ medium. A+ medium is a saline solution composed of several trace elements described in Stevens, et al. (1973) as medium A and supplemented by vitamin B12 at a final concentration of 50 µg/ml and 0.78 g/L $NaNO_3$ unless otherwise stated.

In order to maintain the different cell lines, *wild type* cells were cultured in 50 ml petri dishes with solid A+ medium containing 1,8 % Bacto™ Agar (BD Biosciences). Whereas the transformant strains were cultured in plates with A+ medium as well but supplemented with the antibiotic spectinomycin in a final concentration of 50 µg/ml. All plates were incubated at 37ºC and constant illumination of 100 µmol/m^2/s for 2-3 days and afterwards stored on a laboratory bench at room temperature with natural diurnal light cycle.

The experiments were conducted in liquid A+ medium. S*ynechococcus* 7002 (*wild type, trcBiBP* and *trcEV*) cells were grown test tubes containing 20 ml liquid A+ medium without antibiotics unless otherwise stated. Tubes were sealed with a foam stopper to assure sterility. The stopper was pierced by an inner tube that contained a stopper out of non-absorbent cotton for sterile gas flow. The inner tubes were connected with a needle to a silicon pipe with a constant flux of air supplemented with 3% (v/v) CO_2 to provide aeration and stirring of the culture by bubbling. Test tubes were placed inside an aquarium water bath at 37ºC under continuous illumination provided by one fluorescent light (Phillips Master TL-D 18W) on the left and one light on the right side (Phillips Master TL-D 18W). (Figure 3)

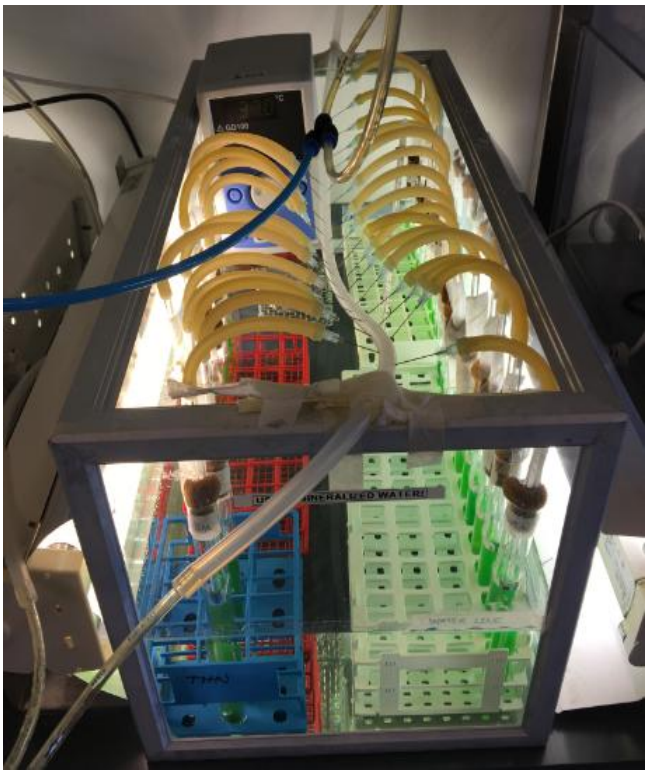

Figure 3: Picture of aquarium tank setup. Synechococcus 7002 wild type, trcEV and trcBiBP were grown in liquid A+ medium with constant illumination and air with 3%(v/v) CO2.

2.4 Experiment 1: Growth and carbohydrate characterisation

Pre-cultures were prepared by transferring colonies from each genotype from plates to 50 ml test tubes filled up to 20 ml with A+ medium supplemented with 50 µg/ml spectinomycin when appropriate. After 18.5 hours growth in the aquarium tank under the previously described conditions, OD_{730nm} measurements and dilutions were conducted to prepare the inoculum for the actual experimental cultures.

The cultures for growth and carbohydrate characterisation were grown in biological triplicates without antibiotics under the previously described conditions. Each biological triplicate had a volume of 80 ml and was distributed over four test tubes. The tubes were distributed in the aquarium tank as shown in figure 4. Four tubes containing only A+ medium were used as negative control, resulting in 40 test tubes in total. Negative controls were placed in another aquarium tank with the same conditions due to space limitations. A schematic representation of experiment 1 can be found in Appendix B.

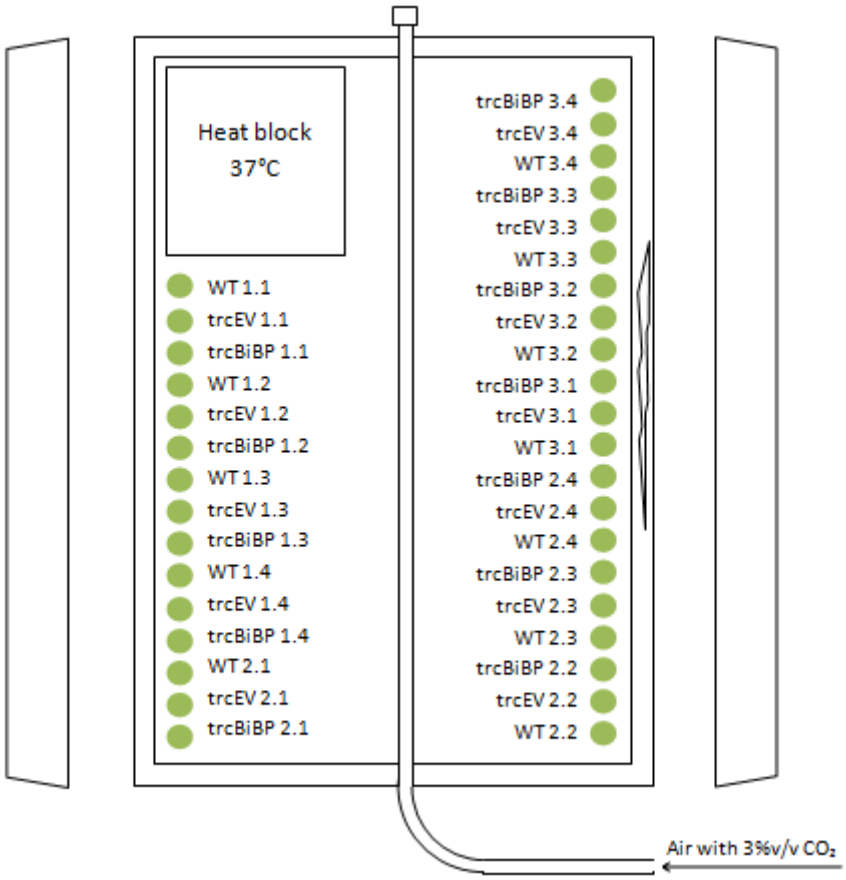

Figure 4: Schematic distribution of test tubes in aquarium tank in experiment 1. The three genotypes were grown in biological triplicates. Each replicate was distributed over four test tubes (e.g. WT1.1, WT1.2, WT1.3 and WT1.4 were later pooled to form WT1).

2.4.1 Characterization of growth

2.4.1.1 Cell density and morphology

Cell growth was monitored by measuring optical density at 730 nm (OD_{730nm}) in a 1 cm light path with a spectrophotometer (Ultrospec 3100 pro, Amersham Biosciences). Cell count and cell physiology of each genotype was studied after growth of 18.5 hours using brightfield microscopy. Samples were diluted 10 times in A+ medium before analysis with microscopy to reduce cell density. Cell number was determined by direct counting in a Neubauer haemocytometer using 20-fold magnification. Cell area and length of cell components were studied using 60-fold magnification with immersion oil and calculated using Image J (http://imagej.nih.gov/ij/).

2.4.1.2 Protein quantification

Pierce BCA Protein Assay Kit was used to quantify total protein cellular content. This method combines the reduction of Cu^{+2} to Cu^{+1} by proteins in an alkaline medium (the biuret reaction) (Kingsley et al. 1939) with the affinity of bicinchoninic acid (BCA) to cuprous cation (Cu^{+1}). The reaction product formed by the chelation of two molecules of BCA with one cuprous ion becomes purple and exhibits an absorbance at 562 nm. This absorbance increases proportionally with increasing protein concentration within a working range of 20-2000 mg/ml.

To perform this assay, BCA working reagent was prepared by mixing 50 parts of BCA reagent A with 1 part of BCA reagent B. After cell disruption which is described in section 2.4.2.1.2, samples were diluted 10 times in MiliQ water and 10 µl were transferred into a 96-well plate. Subsequently, 200 µl of working reagent were added to each well and the plate was shaken by hand for 20 seconds. Afterwards, the plate was covered from light and incubated at 37ºC for 30 minutes. Once the incubation was done, the plate was cooled down to room temperature and the absorbance was measured at 562 nm with a plate reader (Spectramax 190, Molecular Devices Corporation). To avoid over-quantification due to absorbance of pigments present in samples, background absorbance was determined by measuring 10x diluted sample with 200ul MiliQ water instead of working reagent. For both measurements, MiliQ water was used as blank. Background measurements were subtracted from the actual sample measurements. Protein concentrations were determined based on a standard curve of bovine serum albumin (BSA) assayed alongside the unknown samples.

2.4.1.3 Nile red staining

Nile red staining was used to detect potential accumulation of lipids. Nile red is a lipophilic dye that, under light excitation at 514 nm, emits magenta fluorescence (525 - 567 nm) in the presence of polar lipids and green fluorescence (648 - 698 nm) in the presence of neutral lipids.

To analyse the cells from the different genotypes, colonies from plates were diluted in 100 µl A+ medium. Subsequently, Nile red was added to the solution in a final concentration of 1000 µg/ml. Glycerol was also added to the mixture in a concentration of 0.1 g/ml to help Nile red to penetrate the cell wall (Rumin et al., 2015). Samples were incubated for 5 minutes in darkness and then 10 µl were transferred to microscopy slides. Cells without Nile Red were used as negative controls.

Microscope slides of each genotype with and without Nile red were analysed with brightfield microscopy and confocal microscopy. Brightfield microscopy light was filtered using the generic filters TRITC (545 - 565 nm), FITC (475 - 490 nm) and DAPI (385 - 400 nm). With confocal microscopy, cells were excited by a laser at the specific wavelength of 514 nm and the emitted fluorescence was collected in two different ranges; 528 - 579 nm and 636 - 670 nm.

2.4.2 Saccharides analysis

2.4.2.1 Processing for carbohydrate analysis

After 18.5 hours growth of *Synechococcus* 7002 as described in section 2.3, the cultures are collected and processed to analyse intra- and extracellular carbohydrates. The processing involves centrifugation, cell disruption, enzymatic hydrolysis and monosaccharide quantification.

2.4.2.1.1 Separation of cell pellet and spent medium

The content of four aquarium tubes was pooled as indicated in Figure 4 to obtain sufficient sample volume for analysis. The Falcon tubes were centrifuged (Allegra X-22R centrifuge, Beckmann Coulter) at 4500 rpm and 4°C for 15 minutes to separate biomass from spent medium. The pellet was resuspended in 3.75 ml MiliQ water and frozen for further analysis. The spent medium was filtered with a 0.45um filter (Q-Max®, cellulose acetate) and frozen for analysis of extracellular carbohydrates.

2.4.2.1.2 Cell disruption

The resuspended pellets were disrupted using zirconium oxide beads (0.15 mm, Next Advance). 0.5 ml sample and 500 mg of zirconium oxide beads (0.15 mm, Next Advance) were added to beads beating tubes (1.5ml, RINO®). The tubes were shaken for 2 minutes at 0.03 kHz and centrifuged (5417C centrifuge, Eppendorf) for 1 minute at 6000 rpm. This step was repeated 5 times until the pellet disappeared. The supernatants of the beads beating tubes originating from the same Falcon were pooled into one 5 ml Eppendorf. Around 2.8 ml of the 3.75 ml could be recovered. The Eppendorfs were frozen for further analysis.

To estimate the disruption efficiency, the amount of chlorophyll was measured before and after disruption. In triplicates, 20 µl of undisrupted cells were mixed with 980 µl ethanol to measure the amount of chlorophyll before disruption. In triplicates, 20 µl of the supernatant from the beads beating tubes were mixed with 980 µl ethanol to measure the chlorophyll after disruption. It is assumed that unbroken cells will precipitate with the zirconium beads and are therefore not present in the supernatant of the beads beating tubes. The Eppendorfs were incubated at 90°C and 700 rpm for 10 minute to extract and dissolve the chlorophyll. Subsequently, the Eppendorfs were centrifuged for 1 minute at 13000 rpm. 300 µl of the supernatant were transferred to a 96-well plate and the absorbance was measured at 666 nm with a spectrophotometer. The disruption efficiency was determined by dividing the absorbance of disrupted cells by the absorbance of undisrupted cells.

2.4.2.2 Analysis of glucose, sucrose, glycogen and cellulose

2.4.2.2.1 First approach: ethanol precipitations

After disruption, the samples were analysed for presence of glucose, sucrose, glycogen and cellulose. The nine Eppendorfs with samples from wild type, trcEV and trcBiBP, as well as the negative control were analysed. Five positive controls were prepared by adding D-(+)-glucose (Sigmaaldrich, >99.5% pure), sucrose (Sigmaaldrich, > 99.5% pure) and glycogen (USB™, oysters, ultrapure) to A+ medium in concentrations varying from 10 to 200 µg/ml.

Separation and analysis of soluble carbohydrates

0.44 ml from samples and controls were transferred to Eppendorf tubes in triplicates and 1.56 ml ethanol was added. The mixture was vortexed and left at -20°C overnight for precipitation of polysaccharides. Subsequently, the Eppendorfs were centrifuged at 14000 rpm for 20 minutes. The supernatant was separated from the pellet by pouring and pipetting. The supernatant ("EtOH Prec 1 sup") was placed in a SpeedVac (Concentrator plus, Eppendorf) (Concentrator plus, Eppendorf) at 45°C overnight to evaporate the ethanol. It was resuspended in 440 µl MiliQ water. To one fraction of the resuspended supernatant, invertase in sodium azide buffer (Sigmaaldrich, Baker's yeast) was added in a final concentration of 10 U/ml. The glucose concentration was quantified with the GOPOD method described in section 2.4.2.2.4.

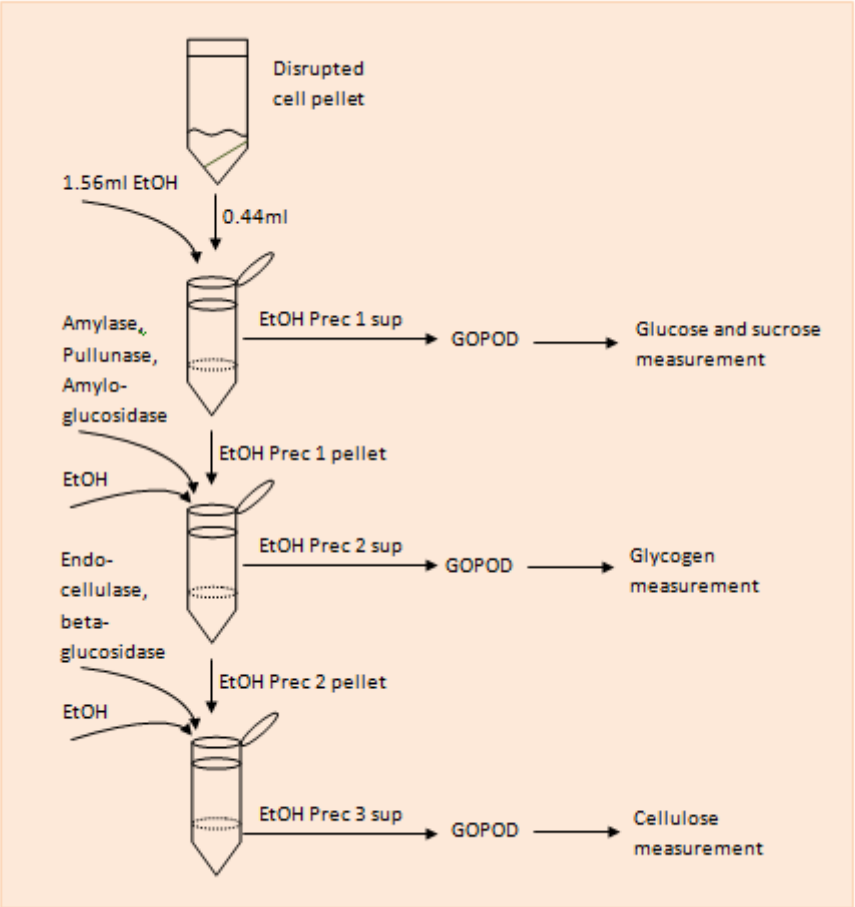

Figure 5: Schematic outline of method 1 for carbohydrate digestion and analysis. Ethanol was added to samples to precipitate polysaccharides and dissolve glucose and sucrose that were subsequently analysed with GOPOD assay. The precipitated polysaccharides glycogen and cellulose are enzymatically digested and the released monosaccharides in the supernatant analysed with GOPOD assay.

The pellet ("EtOH Prec 1 pellet") was airdried to avoid overdrying and resuspended in 440 µl sodium azide buffer by vortexing and ultrasonication (20kHz, Q700, QSonica) at 100% amplitude for 30 s at and stored in the freezer.

Separation and analysis of polysaccharides/glycogen and cellulose

With the EtOH Prec 1 pellet, a second ethanol precipitation was conducted. First, amylase (Megazyme, 3000 U/ml, LOT: 120701b) and pullunase (Megazyme, 700U/ml, LOT: 130103b) were added in a final reaction concentration of 4 U/ml in 2 ml screw cap tubes (Sarstedt). The reactions were incubated for 2 hours at 60°C. 1.56 ml ethanol was added and the tubes were placed at -20°C overnight to dissolve the mono- and oligosaccharides released from glycogen digestion. The tubes were centrifuged for 20 minutes at 13000 rpm. Supernatant and pellet were separated and resuspended as described previously. The supernatant contained the mono- and disaccharides released from glycogen with amylase and pullunase. To convert the disaccharides into glucose, amyloglucosidase (Megazyme, 36U/mg) was added in a final reaction concentration of 1 U/ml and the samples are incubated for 2 hours at 40°C. The released glucose was quantified with the GOPOD method.

A third ethanol precipitation was conducted with the EtOH Prec2 pellet. First, endocellulase (Sigmaaldrich, A.niger, 0.45 U/mg) was added in a final reaction concentration of 0.8 U/ml and the reactions were incubated at 37°C for 2 hours. After addition of ethanol and collection of the supernatant containing oligosaccharides released from cellulose, beta glucosidase (Megazyme, A.niger, 40 U/ml) was added in a final reaction concentration of 0.8 U/ml. The reactions were incubated for 2 hours at 40°C and analysed with GOPOD assay.

2.4.2.2.2 Revision and testing of carbohydrates analysis method

As will be described in more detail in the results chapter, after application of the previously described method, the detected concentrations in samples and controls were lower than expected. This was indicating that something in the separation or quantification process was causing a too low detection of glucose. To identify and eliminate the cause for this, the original method was adapted in two ways and the three methods were tested and compared. The comparison was based on analysing the glycogen content of one sample per genotype, one negative control and the five positive controls prepared, as stated in section 2.4.2.2.1, in duplicates.

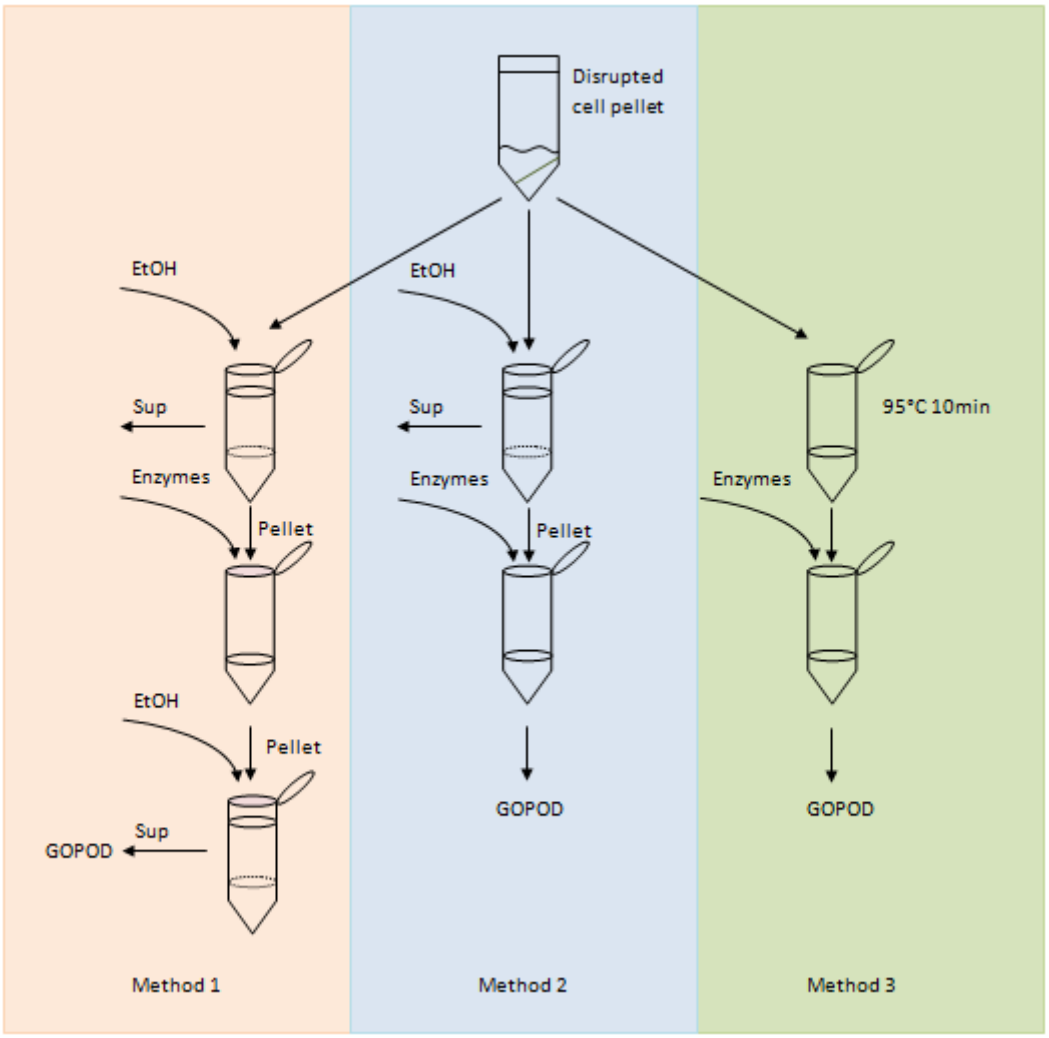

Figure 6: Schematic overview of testing three different methods. Method 1 (orange/left): glycogen is analysed from the supernatant of the second ethanol precipitation. Method 2 (blue/middle): glycogen is digested and analysed in the resuspension of the ethanol precipitation 1 pellet. Method 3 (green/right): glycogen is digested and analysed directly in the sample.

Method 1

The first method is the one described previously. For the testing, only glycogen was digested and analysed and the other measurements were omitted. Glycogen was quantified by measuring the glucose in the supernatant of the second ethanol precipitation with a GOPOD assay as shown in Figure 6.

Method 2

The second method began with the same steps as the first method, including the first ethanol precipitation, ultrasonication of the EtOH Prec 1 pellets and the enzymatic hydrolysis of glycogen. However, after enzymatic hydrolysis, the glucose released from glycogen was directly analysed with a GOPOD assay instead of adding ethanol and dissolving glucose in it. The samples were centrifuged before adding to the 96-well-plate to avoid disturbance of the absorbance measurement by floating particles, assuming that glucose does not precipitate.

Method 3

In the third method, no ethanol precipitations were used. The samples were heated at 95°C for 10 minutes to deactivate proteases that could inhibit the enzymes. Just as in method 2, glycogen was digested and the released glucose directly quantified with a GOPOD assay.

2.4.2.2.3 Final approach of carbohydrates analysis

As described in further detail in the results and discussion, method 3 detected the most glycogen in the samples and controls. Therefore, growth and processing were repeated and the carbohydrates were analysed with the revised method that is described in detail in the following.

The disrupted cells were heated at 95°C for 10 minutes. As shown in Figure 7, the sample volume was divided in order to digest and analyse each carbohydrate separately. Either sodium azide buffer with the respective enzymes or only the buffer was added to the samples in a 1:3 dilution. To analyse free glucose, only sodium azide buffer was added. For sucrose quantification, invertase in sodium azide was added in a final reaction concentration of 10 U/ml. To quantify glycogen, sodium azide containing amylase, pullunase and amyloglucosidase was added to the samples in reaction concentrations of 4, 4 and 1 U/ml, respectively. For glycogen digestion, the reactions were incubated at 50°C for 2 hours and 1000 rpm. To digest and analyse cellulose, endo-cellulase and beta-glucosidase in sodium azide were added in a final concentration of 0.8 U/ml and incubated at 37°C and 1000 rpm for 2 hours. The calculations to determine the absorbance solely caused by the carbohydrate of interest and not by background absorbance are elaborated in section 2.4.2.2.4.

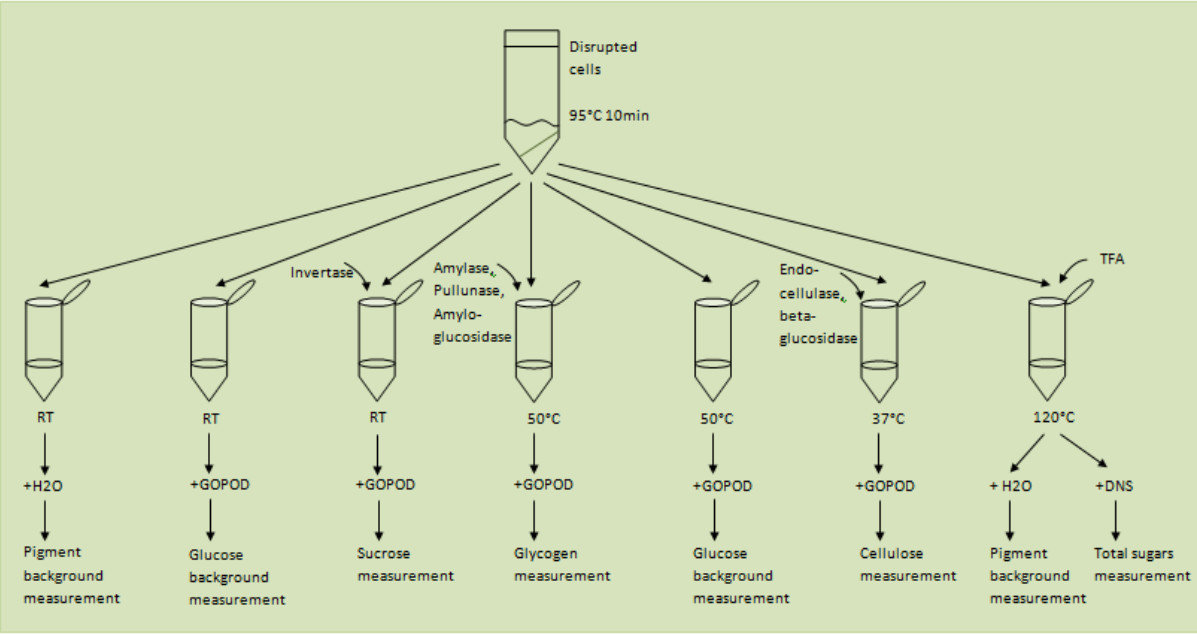

Figure 7: Schematic outline of method 3 for carbohydrate digestion and analysis. Disrupted cells were heated for 10 minutes at 95°C and subsequently divided to digest and analyse each carbohydrate separately. The respective enzymes were added and the reactions incubated at the appropriate temperature. Buffer without enzymes was added to tubes used to measure background glucose and pigments and the tubes incubated in the same way as the respective measurement.

2.4.2.2.4 GOPOD assay

GOPOD is a colorimetric assay to quantify free D-glucose in a solution with two enzymes, glucose oxidase (GO) and peroxidase (POD) as shown below. Presence of glucose in the sample causes formation of quinoneimine dye which changes from colourless to pink proportionally to the amount of glucose present.

$$\text{D-Glucose} + O_2 + H_2O \rightarrow \text{D-gluconate} + H_2O_2 \quad \text{(GO)}$$

$$2\ H_2O_2 + \text{p-hydroxybenzoic acid} + \text{4-aminoantipyrine} \rightarrow \text{quinoneimine dye} + 4\ H_2O \quad \text{(POD)}$$

The detection limit is 0.100 g/L (Data booklet D-Glucose Assay Kit (GOPOD Format), Megazyme). 100 µl sample was transferred to a 96-well plate, 150 µl GOPOD was added and the absorbance at 510 nm was measured after exactly 30 minutes reaction time. The glucose concentration was extrapolated from the absorbances of standards of D-(+)-glucose dissolved in A+ modified medium from which a blank of medium is subtracted.

Measurements and calculations

The absorbance value obtained from the GOPOD assay was not directly corresponding to the carbohydrate of interest due to the fact that other compounds add up to the absorbance value such as pigments, background glucose, the enzyme solution and the GOPOD reagent itself. To determine the absorbance solely caused by the carbohydrate of interest, background absorbances were measured in separate assays and subtracted from the total absorbance value. Depending on the type of carbohydrate and sample analysed, this background value was derived differently which is elaborated in more detail in the following sections. From each absorbance value, a blank is subtracted. The blank consisted of water that was processed in the same way as the samples in the specific assay. Each concentration was divided by the OD_{730} of the respective biological replicate for standardization.

Measurement and calculation of glucose

To analyse the free glucose concentration in the sample, the absorbance of 100 µl sample with 150 µl GOPOD is determined. This absorbance was corrected by the absorbance caused by pigments by measuring 100 µl sample with 150 µl water instead of GOPOD.

$$\text{Abs}_{\text{glucose}} = (\text{Abs}_{\text{glucose assay}} - \text{Abs}_{\text{glucose assay blank}}) - (\text{Abs}_{\text{pigment background assay}} - \text{Abs}_{\text{pigment background assay blank}})$$

Measurement and calculation of sucrose, glycogen and cellulose

For analysis of sucrose, glycogen and cellulose, the carbohydrate assay measured the amount of glucose present after treatment with enzymes. Samples without addition of enzymes were incubated and analysed with GOPOD and used to subtract glucose and pigment background simultaneously. For the sucrose assay, sucrose standards were used as standard curve because the conversion of sucrose into glucose and fructose catalysed by invertase is an equilibrium reaction. Glycogen standards were used as positive controls for the enzymatic digestion in the glycogen assay. Cellulose (Sigmaaldrich, microcrystalline) standards were used as positive control for the enzymatic digestion in the cellulose assay.

$Abs_{di-/polysaccharide} = (Abs_{di-/polysaccharide\ assay} - Abs_{di-/polysaccharide\ assay\ blank}) - (Abs_{glucose\ background\ assay} - Abs_{glucose\ background\ assay\ blank})$

For each assay, first a test round without technical replicates was conducted in order to determine the required dilution to reach the sensitivity range of the GOPOD assay. Subsequently, the actual assay was conducted in technical triplicates. The concentrations of carbohydrates were standardized by dividing by the OD_{730nm} of the cell culture of the respective biological replicate.

2.4.2.3 Analysis of total sugars

2.4.2.3.1 TFA hydrolysis and DNS assay

For estimation of total reducing sugars, the samples were treated with 4M trifluoroacetic acid (TFA) (Sigmaaldrich, 99%) in duplicates and subsequently analysed with a 3,5-Dinitrosalicylic acid (DNS) assay. DNS reagent was prepared as described in the following: 10 g of 3,4 dinitrosalycilic acid was dissolved in 200 ml MiliQ water and mixed with 200 ml 2 M NaOH. The mixture was heated to 50°C and 403 g of sodium potassium tartrate (Rochelle salt) are slowly added. The volume was made up to 1.0 L with distilled water. Five different standards of 0.5 to 10 g/l glucose in medium served as positive controls. Water instead of sample was used as blank. 325 µl 4M TFA was added to 325 µl each sample, standard and blank and incubated at 120°C for 2 hours. The tubes were centrifuged at 14000 rpm for 5 minutes and 600 µl of the supernatant was placed in a SpeedVac at 45°C overnight to evaporate the TFA. The pellets from the SpeedVac were resuspended in 60 µl 50 mM sodium acetate buffer (pH=4.5) to be 5 times concentrated. The resuspension was distributed over two tubes. 300 µl DNS was added to the first tubes for total reducing sugars measurement. 300 µl MiliQ water was added to the second tubes for pigment background measurement. To obtain a standard curve, 15 µl standard was diluted with 15 µl buffer and 300 µl DNS was added. The tubes were incubated at 100°C for 15 minutes. Subsequently, 300 µl was transferred to a 96 well plate and the absorbance was read at 540 nm. The absorbance caused solely by the reducing sugars is calculated in the following way:

$Abs_{total\ reducing\ sugars} = (Abs_{total\ reducing\ sugars\ assay} - Abs_{total\ reducing\ sugars\ assay\ blank}) - (Abs_{pigment\ background\ assay} - Abs_{pigment\ background\ assay\ blank})$

For each DNS assay, first a test round with one measurement per biological replicate is conducted in order to determine the required dilution to reach the sensitivity range of the DNS assay. The actual assay is then conducted in technical duplicates. The concentrations of total sugars were standardized by dividing by the OD_{730nm} of the cell culture of the respective biological replicate.

2.5 Experiment 2: Effect of position in aquarium tank on growth

Experiment 2 was conducted to study the growth of wild type and trcBiBP on different positions in the aquarium tank. Pre-cultures of wild type and trcBiBP were prepared in the same way as described in section 2.3, serving as inoculum for six tubes per genotype. The inoculum was diluted with A+ medium to a starting OD_{730} of 0.055. Two tubes with A+ medium were used as negative control.

Duplicates of wild type and trcBiBP were placed at the left side, the right side and behind residues of a former plastic light shading at the right side of the aquarium. The same growth conditions as described in section 2.3 were applied. OD_{730} of the 14 tubes was measured over a duration of 115 hours. 1 ml sample was collected from each tube under sterile conditions. The samples were diluted as appropriate to fit the sensitivity range of 0.1 to 0.9 of the spectrophotometer. Each sample was measured three times and the average calculated and used for the growth curve. For calculation of doubling times, only OD_{730} in the range of 0.1 and 0.7 were taking into consideration (De Porcellinis et al., 2018). Doubling times were calculated with the following formula:

$$t\ 1/2 = \frac{growth\ duration\ (h)\ \times\ log\ (2)}{log\left(final\ OD\ \times \frac{cell\ count}{OD}\right) - log\left(initial\ OD\ \times \frac{cell\ count}{OD}\right)}$$

The light intensity was measured with a universal light intensity meter (ULM-500, Walz). For light intensity measurement, the sensor was placed in an empty test tube to measure each point in the aquarium tank where culture tubes can be positioned. The average of the light intensity of each of the three different positions (left, right, right plastic) was calculated for comparison. A schematic representation of experiment 2 can be found in Appendix C.

2.6 Experiment 3: Effect of initial $NaNO_3$ concentration on growth and glycogen content

In experiment 3, the effect of different $NaNO_3$ concentrations in the A+ medium on $OD_{730nm,}$ protein and glycogen content was studied. Pre-cultures of wild type and trcBiBP were prepared in the same way as described in section 2.3, serving as inoculum for six tubes per genotype with a starting OD_{730nm} of 0.055. Three different types of A+ medium with 0.28 (N-), 0.78 (N) and 1.28 (N+) g/L $NaNO_3$ were prepared. wild type and trcBiBP were grown in the three different media in duplicates. One tube per type of medium was prepared as negative control. The tubes were placed at the right side of the aquarium. The same growth conditions as described in section 2.3 were applied. After 18.5 hours growth duration, OD_{730} of the 14 tubes was measured. The samples were diluted as appropriate to fit the sensitivity range of 0.1 to 0.9 of the spectrophotometer. The cultures were processed and the protein and glycogen content quantified as described in section 2.4.2. A schematic representation of experiment 3 can be found in Appendix D.

2.7 Statistical analysis

Student's test assuming unequal variances was performed in Microsoft Excel to analyse the data. Only *P*-values ≤ 0.05 were considered statistically significant.

3 Results

3.1 Transformation of Synechococcus 7002

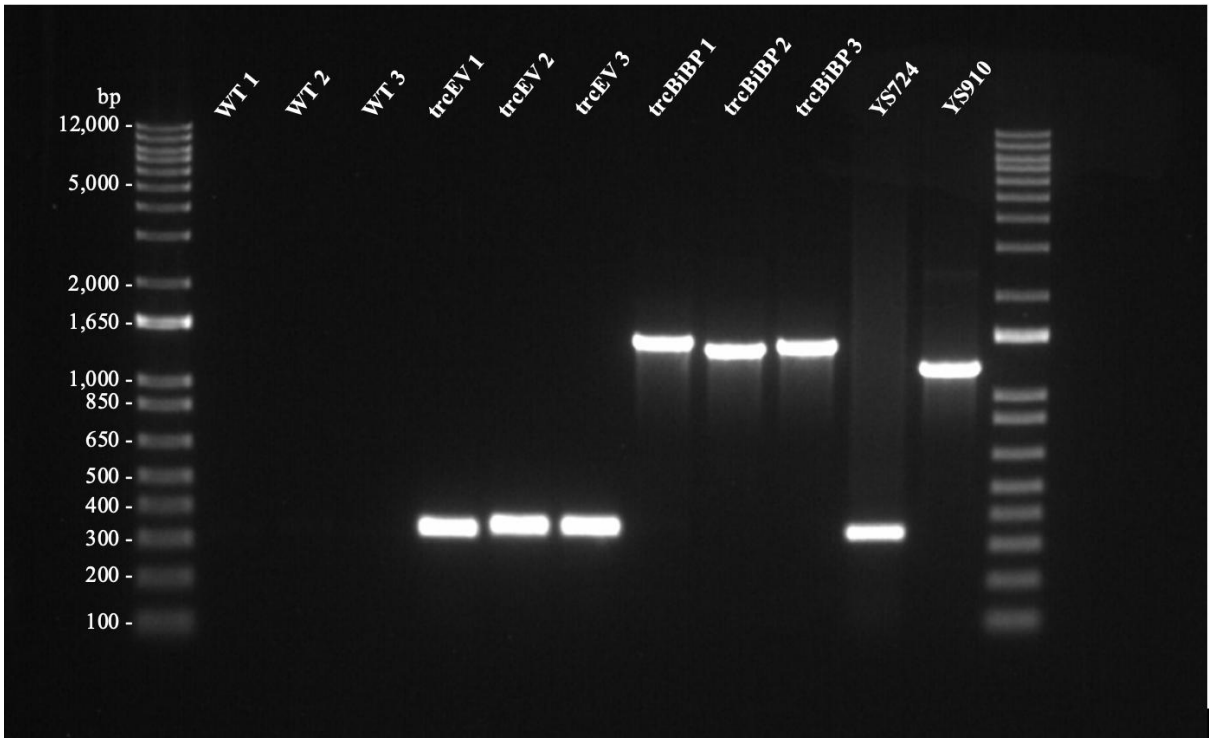

Figure 8: Gel electrophoresis of PCR amplified products using specific primers. Lanes 1-3 correspond to examined Synechococcus 7002 wild type cells, lanes 4-6 to trcBiBP, lanes 7-9 to trcEV and lanes 10 and 11 to E. coli YS724 and YS910 strains respectively. 1 kb plus DNA size marker in both sides of the gel.

As shown in Figure 8, a band of around 1,300 bp was visible in *trcBiBP* samples. This band had the same size than the one obtained in YS910; *E. coli* strain used to transfer the *pDF-trcBiBP* vector to *Synechococcus* 7002. Another band of around 300 bp was visible in *trcEV* samples and YS724; *E. coli* strain used to transfer the *pDF-trcEV* to *Synechococcus* 7002. Besides, no band was found in any of the *wild type* replicates.

These results were consistent with the observation that both transgenes, *trcBiBP* and *trcEV* grew on plates with spectinomycin (50 mg/ml) and therefore had incorporated the respective plasmid with the resistance to this antibiotic, whereas no growth of *wild type* was found in plates with antibiotic.

3.2 Experiment 1: Growth and saccharide characterization

3.2.1 Cell size

The overexpression of BiBPase lead to physiological differences between *wild type* and *trcBiBP*. The study of the three different genotypes with brightfield microscopy show that *trcBiBP* cells were visibly larger than *wild type* cells (Figure 9). Image J results compiled in Table 1 showed an average cell area of *wild type* cells of 3.52 μm^2, whereas *trcBiBP* cells had an average area of 5.66 μm^2.

However, *trcEV* cells also happened to be bigger than *wild type* cells with an average area of 4.13 μm^2. Both differences were confirmed by statistical significance. ($P < 0.05$; n = 118)

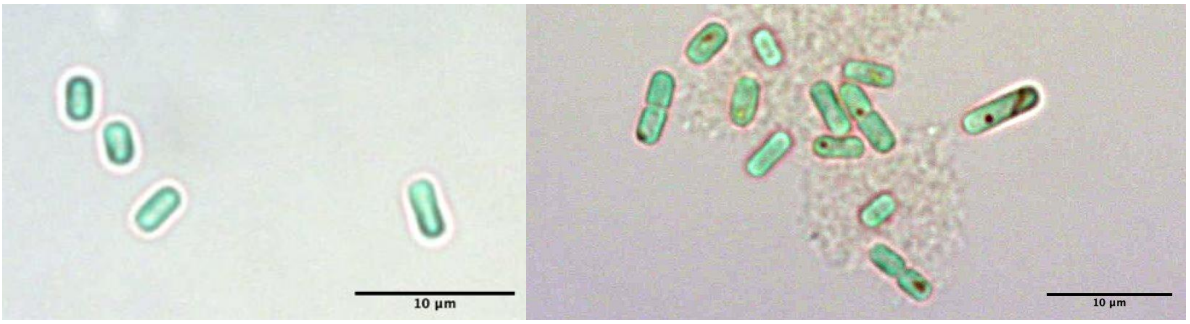

Figure 9: Pictures of Synechococcus 7002. Images taken with brightfield microscopy at 60-fold magnification with immersion oil. Wild type cells on the left side and trcBiBP on the right.

OD

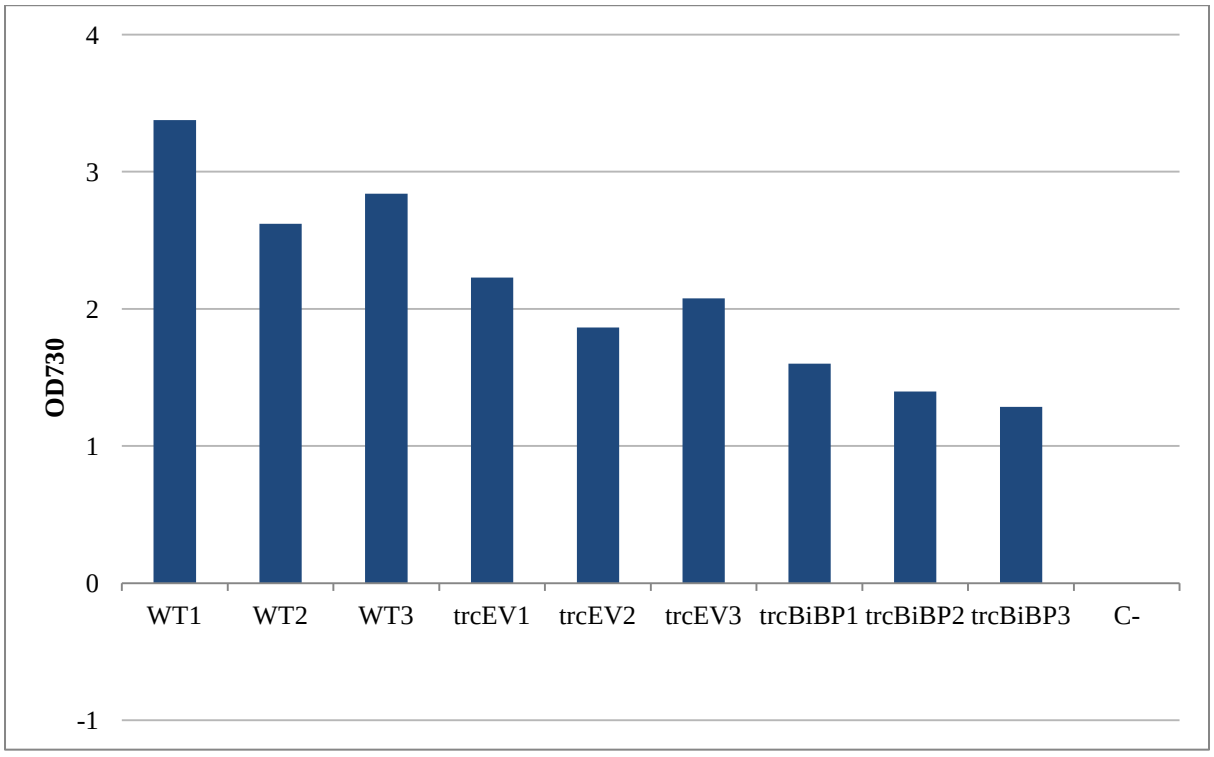

Figure 10: OD_{730nm} measurements of the different biological replicates obtained after 18.5 hours cultivation under set up conditions.

Growth differences after 18.5 hours of cultivation were quantified by OD_{730nm} and displayed in Figure 10. Regarding each genotype individually, it can be observed that the replicant number 1 of each genotype had always slightly higher ODs compared to the other two. On average, *wild type* cultures had higher ODs compared to both transgenic strains. Whereas, *trcBiBP* showed lower OD measurements in all replicates. The average OD values per genotype can be found in Table 1. Difference between all genotypes were statistically significant ($P < 0.05$; n = 3).

3.2.2 Cell count per OD

Regarding cell count of the different genotypes, differences were observed between *wild type* and *trcBiBP*. Cell count was expressed per OD_{730nm} and data can be found in Table 1**.** Table 1 shows a higher number of *wild type* cells per OD compared to the transgenic stain *trcBiBP* and this difference was statistically significant. ($P < 0.05$; $n = 3$) Whereas the difference in cell count per OD_{730nm} between *wild type* and *trcEV* was not statistically significant. ($P > 0.05$; $n = 3$)

Strain	**Area (μm^2)**	**Cell count/ml ($x10^7$)**	**OD_{730nm}**	**cell count/OD_{730nm} ($x10^7/OD_{730nm}$)**
wild type	3.52 ±0.9	28.83 ±9.1	2.95 ±0.4	9.66 ±1.9
trcEV	4.13 ±2.2	14.52 ±3.6	2.06 ±0.2	7.05 ±1.5
trcBiBP	5.66 ±0.9	9.31 ±0.8	1.43 ±0.2	6.56 ±7.0

Table 1: Physiological characteristics of wild type, trcEV and trcBiBP strains of Synechococcus 7002. Area measurements were calculated with ImageJ analyzing 118 wild type cells, 165 trcEV cells and 318 trcBiBP cells. Mean and standard deviations of cell count and OD were obtained from biological triplicates of each genotype. Cultures were grown in liquid media as described in section 2.3.

3.2.3 Protein quantification

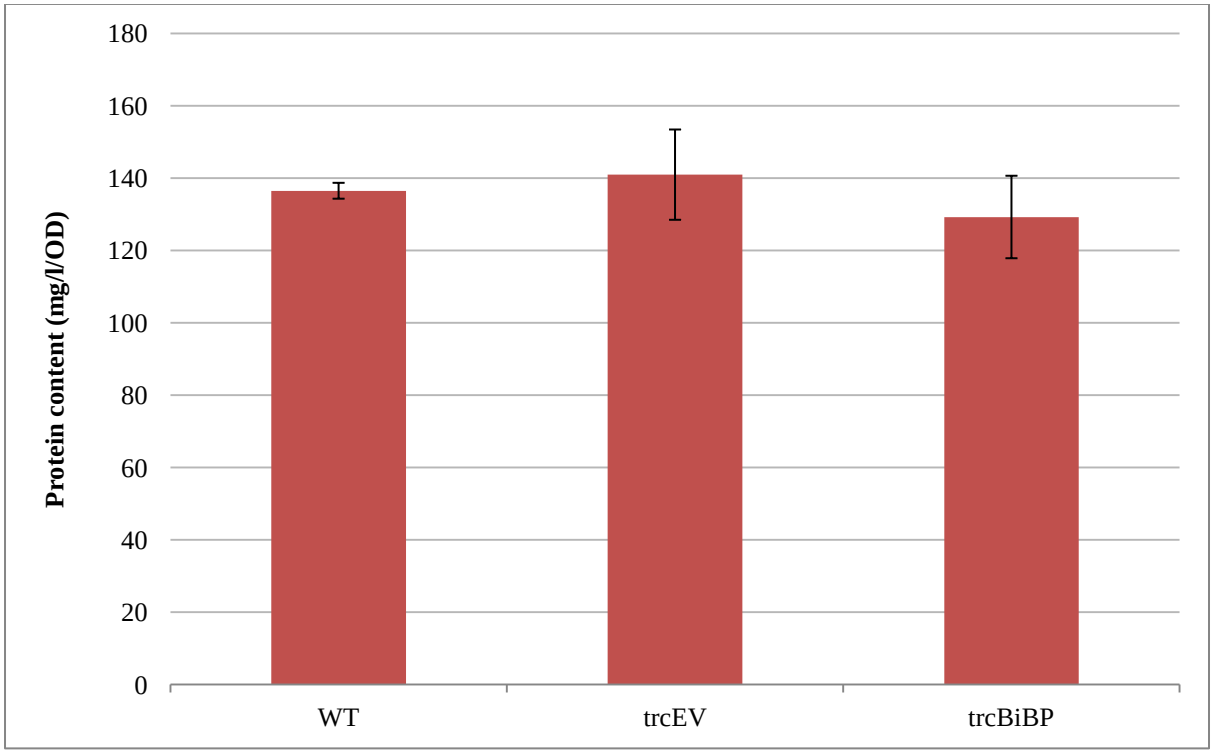

Figure 11: Total protein content of the three genotypes (wild type, trcEV, trcBiBP) expressed mg/l and standardized per OD. Error bars show standard deviation between the three biological replicates.

Results of protein quantification by BCA assay are summarized in Figure 11. This graph combines the average of the biological triplicate of the different genotypes. Total protein content of all genotypes appears to be very similar. *TrcEV* cells had higher protein content with a total amount of 141 mg/l/OD_{730nm} and *trcBiBP* had the least with 129 mg/l/OD_{730nm} total proteins. These differences were confirmed to be not statistically significant. ($P > 0.05$; n = 3)

3.2.4 Nile red staining

Analysing the cells of the different genotypes under brightfield microscopy an unusual artefact was found in *trcBiBP* cells (Figure 9). This artefact was found in 21% of *trcBiBP* cells and in none of the *wild type* or *trcEV* cells. Only one artefact was found per cell and it appeared like one black dot that turned yellow when the focus was changed. The observation of these artefacts was consistent when the transformation was reproduced. The artefact had a diameter of 703 ± 33nm. In order to determine if this artefacts represent an accumulation of lipids, Nile red staining was conducted.

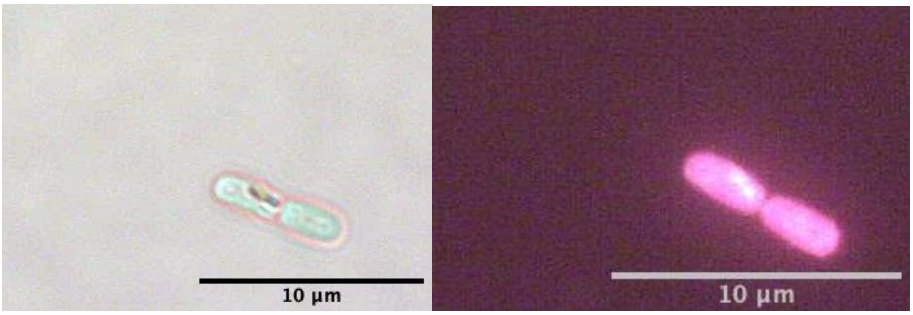

Figure 12: Pictures of trcBiBP stained with Nile red. On the left; trcBiBP cell on brightfield microscopy. On the right; same trcBiBP cell on brightfield microscopy with fluorescence collected under TRITC filter (545 - 565 nm).

The analysis with the brightfeld microscopy of trcBiBP cells revealed fluorescence in cells with and without Nile Red staining. The fluorescence in cells with Nile Red was visibly higher than in cells without Nile Red. Collecting the emitted light with a TRITC filter (545 - 565nm) showed fluorescence in the whole cell. As shown in Figure 12, the artefact appeared to be more fluorescent than the rest of the cytoplasm. Confocal microscopy was used to distinguish the emitted fluorescences in artefact and cytoplasm, for instance coming from chlorophyll by wavelength.

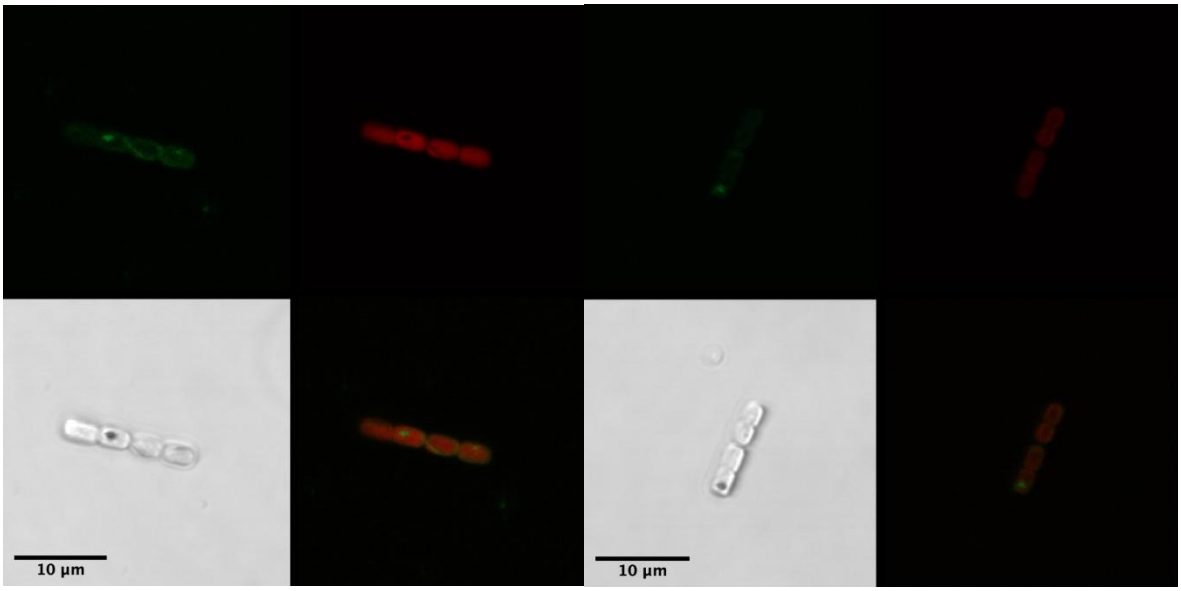

Figure 13: Pictures of trcBiBP cells taken with confocal microscopy. On the left; trc*BiBP cells stained with Nile Red, and on the right;* trc*BiBP cells without Nile Red. In all the pictures cells were excited with a single wavelength of 514 nm but light was collected at different wavelengths in the different sections. On the top left section of each picture, light was collected between 528 - 579 nm wavelengths and coloured green, on the top right between 636 - 670 nm and coloured red. Bottom left section corresponds to an outline of cell in black and white and bottom right the sum of both fluorescents collected.*

As presented in Figure 13, confocal microscopy revealed that the excitation at 514 nm of *trcBiBP* cells stained with Nile red (left picture) resulted in fluorescence in both of the different wavelength ranges collected. In the range of 528 - 579 nm (top left section) low emission is found dispersed in the cytoplasm whereas a higher emission if observed on the small section corresponding to the position of the artefact. In contrast, in the range of 636 - 670 nm (top right section) high levels of fluorescence are detected everywhere in the cytoplasm except for the section corresponding to the artefact, where no fluorescence seems to be detected. The same tendency was found when mutant cells without Nile red (right picture) were analysed. However, since both pictures were taken under the same fluorescence gain setting, we can state that the fluorescence by cells without Nile red was lower than the emitted from cells stained with Nile red.

3.3 Processing

3.3.1 Cell disruption efficiency

The chlorophyll measurements showed disruption efficiencies between 105 and 119% with an average of 114 ± 7%. The disruption efficiencies for the triplicates of wild type, EV and trcBiBP were 118 ± 1.5%, 112 ± 6% and 113 ± 5%.

3.4 Saccharide analysis

As mentioned in section 2.4.2.2.2, a first round of experiments was conducted with enzymatic hydrolysis and ethanol precipitations as method to quantify the different carbohydrates. The detected concentrations in the positive controls were 12-56% of the initially added concentrations. Therefore, the method has been adapted in two different ways and the three methods were tested for comparison of release of glucose from glycogen.

3.4.1 Method testing

The testing of the three different methods showed that method 1 detected the lowest glycogen content in samples and the least accurate estimation of the positive controls. According to method 1, the glycogen concentrations in the samples showed little difference between the genotypes with values between 0.58 and 0.66 mg/L and with the highest concentration in wild type and the lowest in trcEV. In contrast to the other methods, the positive controls showed an inconsistent trendline. Method 2 detected more glycogen in samples and positive controls but also in negative control than method 1. Method 3 detected the most accurate glycogen concentration in the positive controls as the results were the closest to the initially prepared concentrations. Method 3 also detected the most glycogen in the samples compared to other methods. According to method 3, trcBiBP showed the highest result of 3.39 mg/l which was almost twice as much as wild type and EV. This trend is consistent with method 2 and contrary to method 1. Glycogen concentrations obtained with each method can be found in Appendix E.

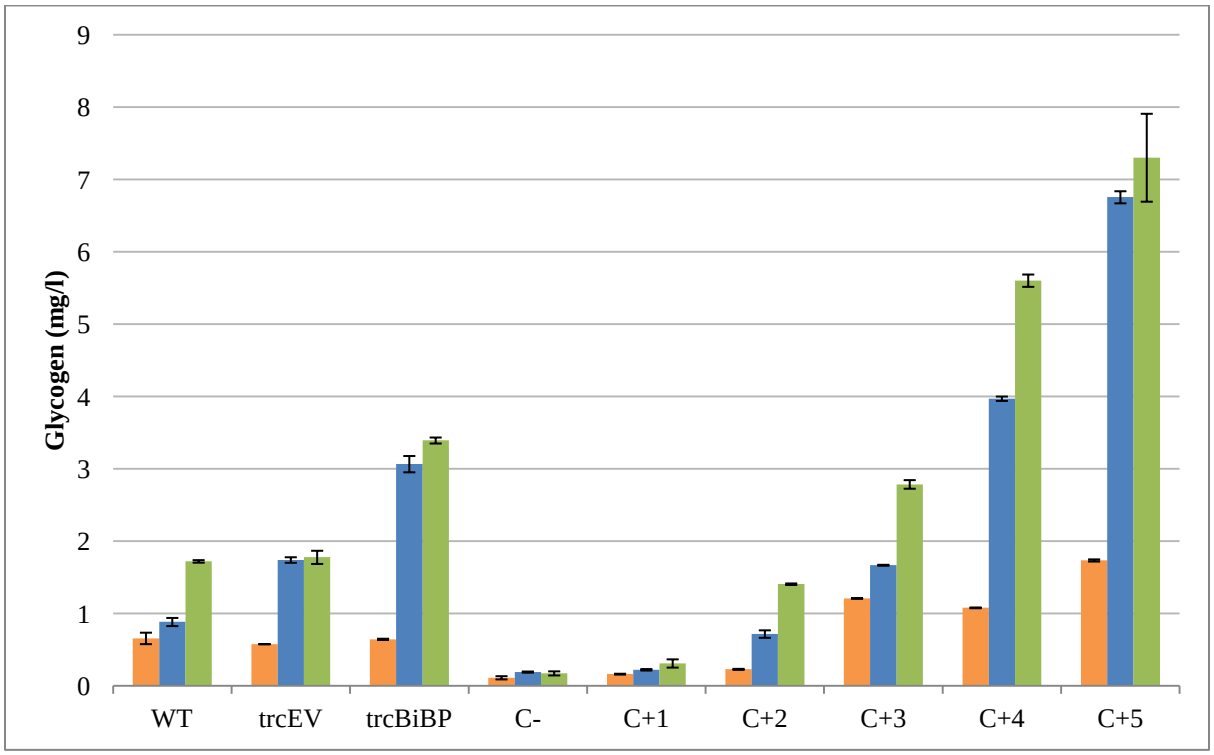

Figure 14: Method testing. Analysis of glucose released from digested glycogen from one sample per genotype (WT, EV, NB), one negative control (C-) and five positive controls (C+1 to C+5) with three different methods. Method 1: three ethanol precipitations, method 2: one ethanol precipitation, method 3: no ethanol precipitations. Error bars showing the standard deviation of the technical duplicates.

3.4.2 Carbohydrates analysis

The carbohydrates of wild type, trcEV and trcBiBP were quantified with the revised method (method 3). Figure 14 depicts the intracellular glycogen, cellulose and glucose content of each biological replicate of the three genotypes individually. Glycogen represented the largest fraction in all genotypes. Regarding the variation between the biological replicates of the same genotype, wild type

and trcEV showed the same trend in detected glycogen and cellulose. The biological replicates of wild type and EV differed greatly with WT1 and trcEV1 showing the highest values in comparison to the other two biological replicates. WT1 showed the highest glycogen content from all samples with 6.00 mg/L/OD. WT2, WT3, trcEV2 and trcEV3 showed similar values of around 0.76 mg/L/OD glycogen and 0.78 mg/L/OD cellulose. The glycogen and cellulose concentrations in trcBiBP were more consistent within the replicates. On average, trcBiBP samples contained 4.54 mg/L/OD glycogen and 2.87 mg/L/OD cellulose. Within the replicates, trcBiBP showed the opposite trend compared to the other genotypes with trcBiBP1 containing slightly lower glycogen and cellulose than the other replicates. Sucrose could not be detected in any of the samples. Glucose measurements were below the detection level with the only exception being WT1 and trcEV1. The specific concentrations of carbohydrates can be found in Appendix F. This experiment has been repeated in order to test the reproducibility of the findings. Inoculation, growth, processing, digestion and analysis were conducted in the same way. The results in the repeated experiment which can be found in the Appendix G showed similar concentrations of glucose, glycogen and cellulose and the same trend of WT1 and trcEV1 containing more glycogen and cellulose than the other biological replicates, as well as the trend in trcBiBP which contained the least glycogen and cellulose in trcBiBP1.

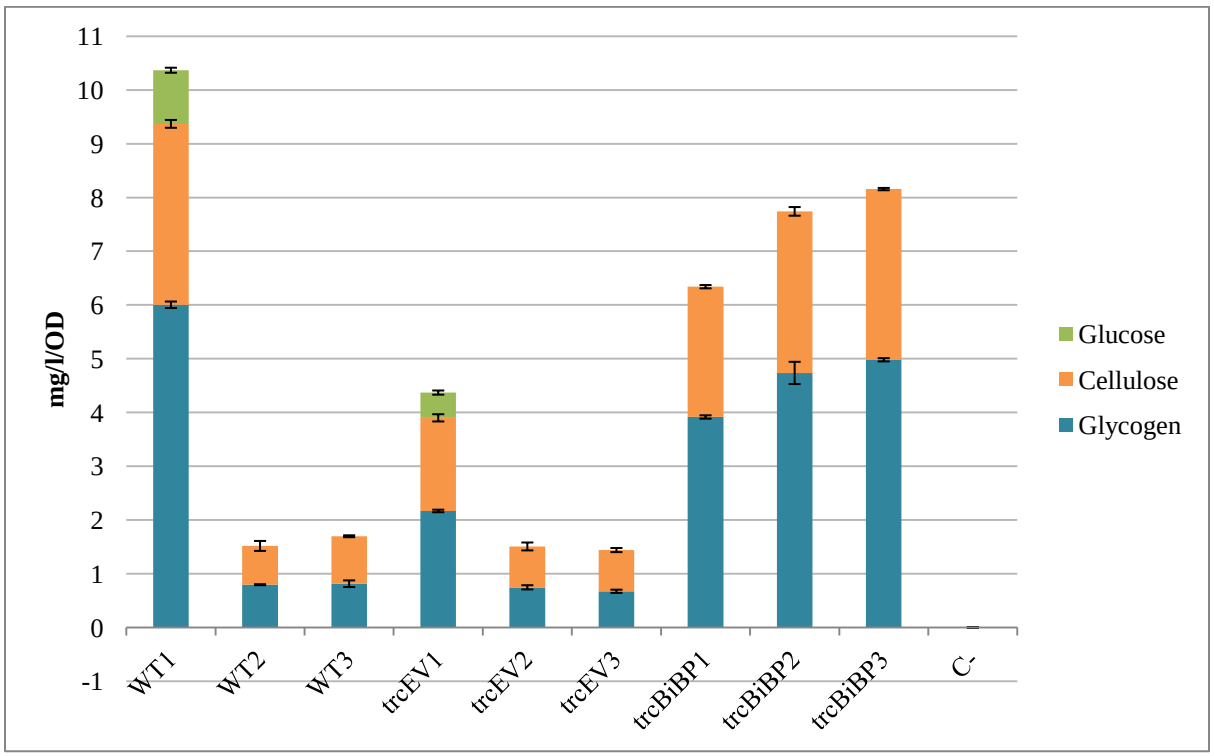

Figure 15: Intracellular carbohydrates analysis; glucose, glycogen and cellulose concentration of the biological triplicates of wild type, trcEV, trcBiBP and C- obtained with GOPOD assay. The error bars show the standard deviation of the technical triplicates. Each value was standardised by dividing by OD.

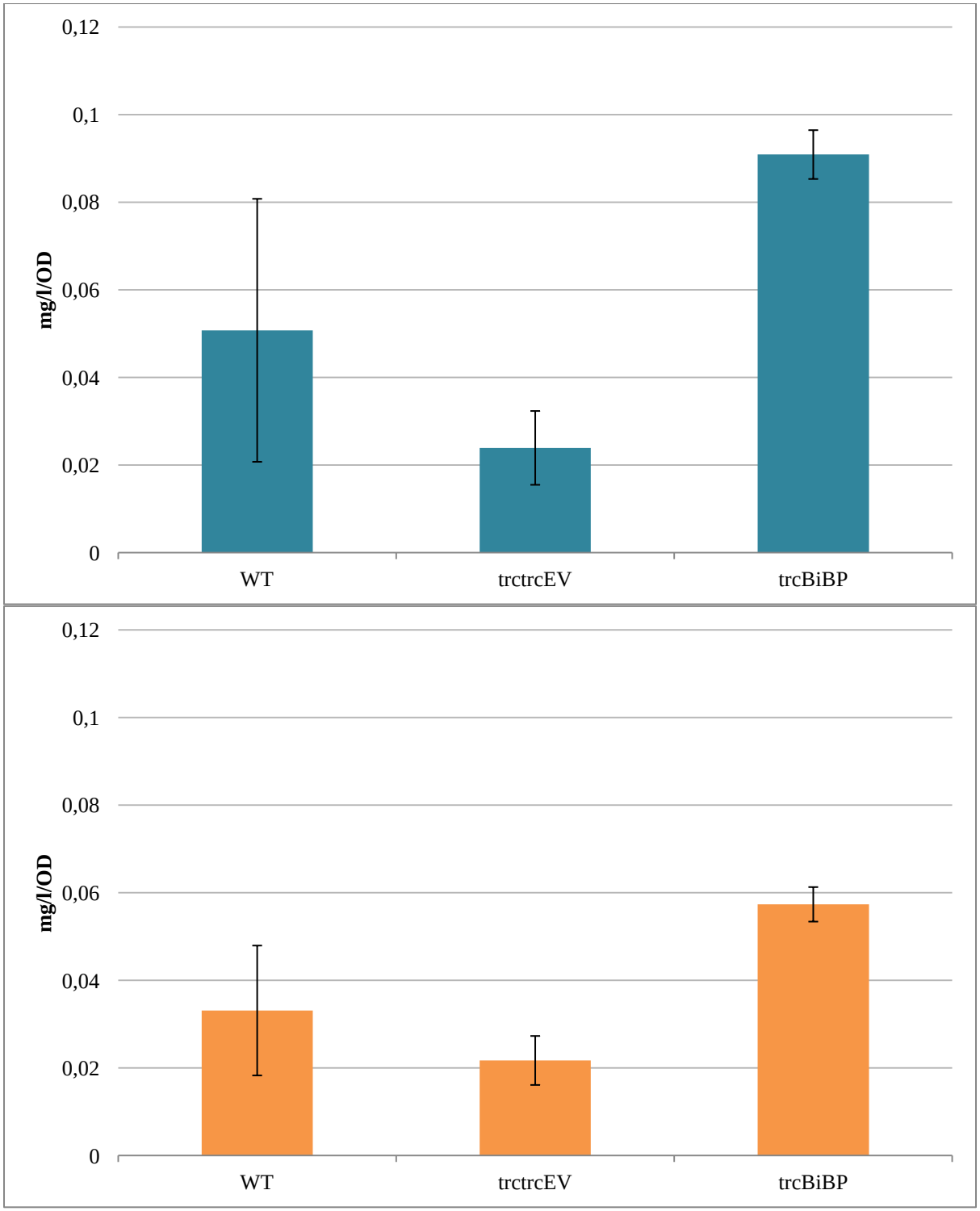

Figure 16: Average intracellular glycogen (top) and cellulose (bottom) content per genotype. Error bars showing the standard deviation of the biological replicates. Each value was standardised by dividing by OD.

Figure 16 shows the average glycogen (top) and cellulose (bottom) content per genotype. All genotypes contained more glycogen than cellulose. Comparing the different genotypes to each other, trcBiBP contained the most glycogen and cellulose whereas trcEV showed the least. wild type and trcEV showed greater variance than trcBiBP due to the variability in the biological replicates as shown in figure 15.

The glycogen and cellulose content of trcBiBP was statistically significantly different from trcEV ($P < 0.05$; $n = 3$) but not from wild type ($P > 0.05$; $n = 3$). This is inconsistent with the repeated experiment in which glycogen and cellulose of trcBiBP was statistically significantly different from both, trcEV and wild type ($P < 0.05$; $n = 3$). However, when the results from both experiments were combined and treated as if they were obtained in the same experiment, trcBiBP was significantly different from wild type and trcEV in glycogen and cellulose ($P < 0.05$; $n = 6$).

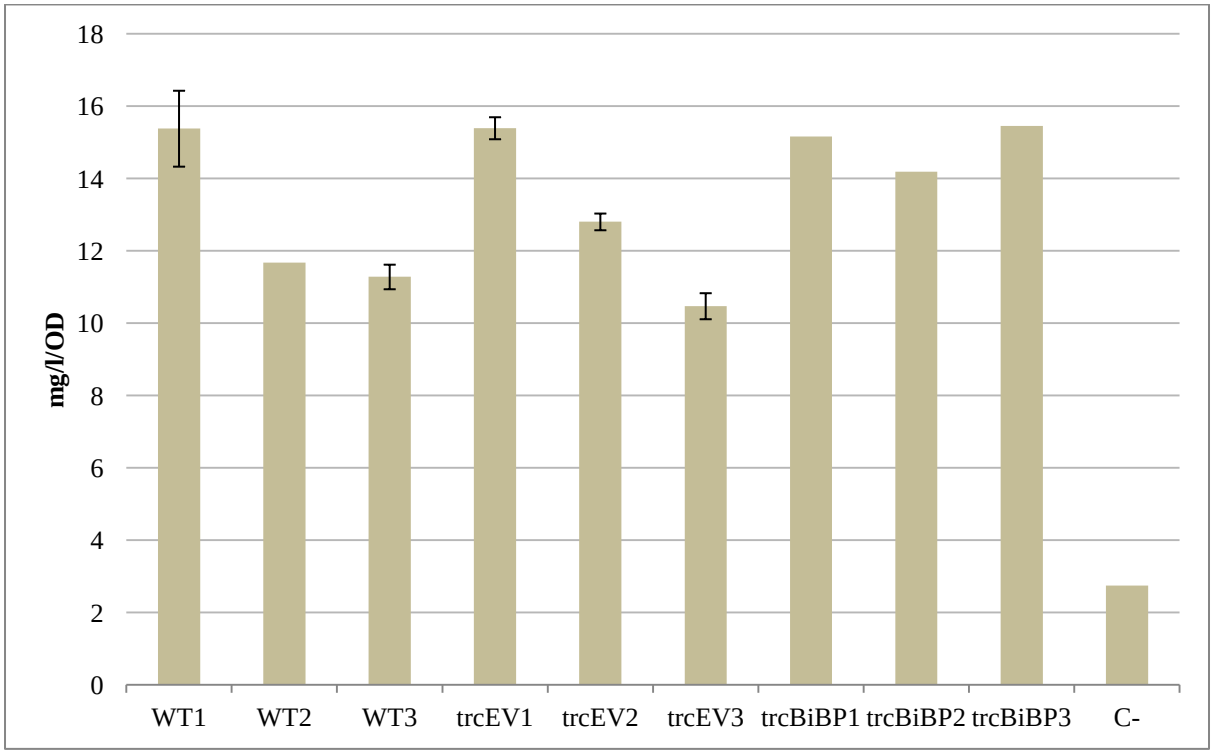

Figure 17: Total reducing sugars of each biological replicate estimated with TFA hydrolysis and DNS assay. Error bars showing the standard deviation of the technical duplicates.

Figure 17 depicts the total intracellular reducing sugars estimated with TFA hydrolysis and DNS assay. Total reducing sugars showed the same trend as glycogen and cellulose in the different genotypes. WT1 and trcEV1 contained more total sugars than WT2, WT3, trcEV2 and trcEV3. TrcBiBP showed the opposite trend with the least sugar content measured in BiBP1 compared to the other two biological replicates. The average total reducing sugar content of wild type, trcEV and trcBiBP were 11.56, 10.12 and 12.71 mg/L/OD, respectively. The difference in total reducing sugars between the genotypes was not statistically significant ($P > 0.05$; $n = 3$).

Extracellular glucose, sucrose and total reducing sugars could not be detected as they were below the detection limits of GOPOD and DNS assay.

3.4.3 Reliability of enzymatic carbohydrate digestion and GOPOD assay

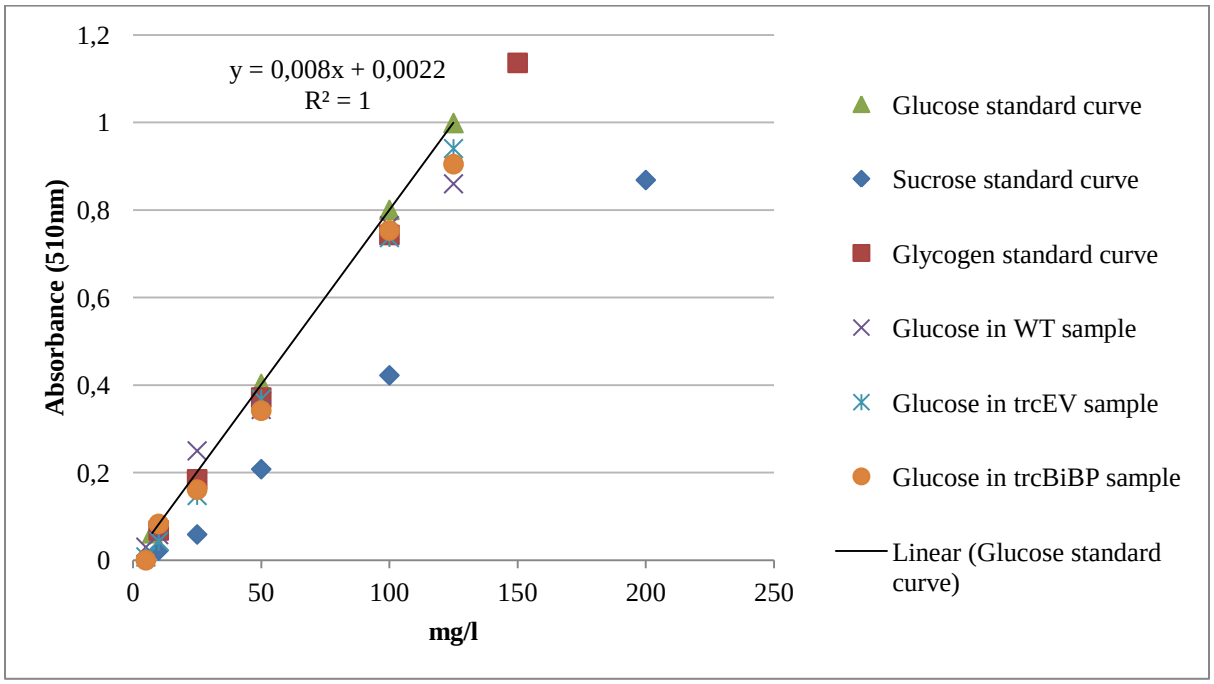

Figure 18: Reliability of enzymatic carbohydrate digestion and GOPOD assay. Absorbances of different types of carbohydrates dissolved in either medium or disrupted cells solution and analysed with GOPOD.

The absorbances of different types of standards after deduction of blanks are shown in Figure 18. The standard curve of glucose dissolved in medium ranging from concentrations from 7.5 mg/L to 125 mg/L showed a R^2 of 1. Glucose added to disrupted cell solutions of wild type, trcEV and trcBiBP showed similar curves to glucose standards prepared in medium. The glucose released from glycogen standards with 4 U/ml amlyase, 4 U/ml pullunase, and 1 U/ml amyloglucosidase was almost equal to the concentration of glycogen in which they have been prepared.

The slope of the sucrose standard curve is lower than the glucose standard curve. Glucose released from microcrystalline cellulose with endo-cellulose and beta-glucosidase was below the detection range and was omitted from Figure 15.

3.5 Experiment 2: Effect of position in aquarium tank on growth

Figure 19 shows the OD_{730} values of wild type and trcBiBP grown at three different positions of the aquarium tank measured over time. The cultures were placed at the left side, the right side and behind residues of a former plastic light shading at the right side of the aquarium. TrcBiBP showed lower OD_{730} values at any position and at any point in time compared to wild type. The doubling time of trcBiBP of ($t_{1/2,\ trcBiBP}$ = 4.34 ± 0.45 hours) was slower than wild type ($t_{1/2,\ wild\ type}$ = 2.6 ± 0.14 hours). The difference in doubling time was statistically significant (P > 0.05; n = 3).

On linear scale it seems as if wild type and trcBiBP were in a lag phase for approximately 10 hours and then continued to grow exponentially for the whole duration of the experiment. On logarithmic scale, it seemed as if the growth velocity of wild type increased until an OD_{730nm} of around 1 and subsequently decreased and wild type started entering the stationary phase around an OD_{730nm} of 5.

The growth velocity of trcBiBP appeared to be lower than wild type, starting to enter the stationary phase at a later point in time but also at an OD_{730nm} of around 5.

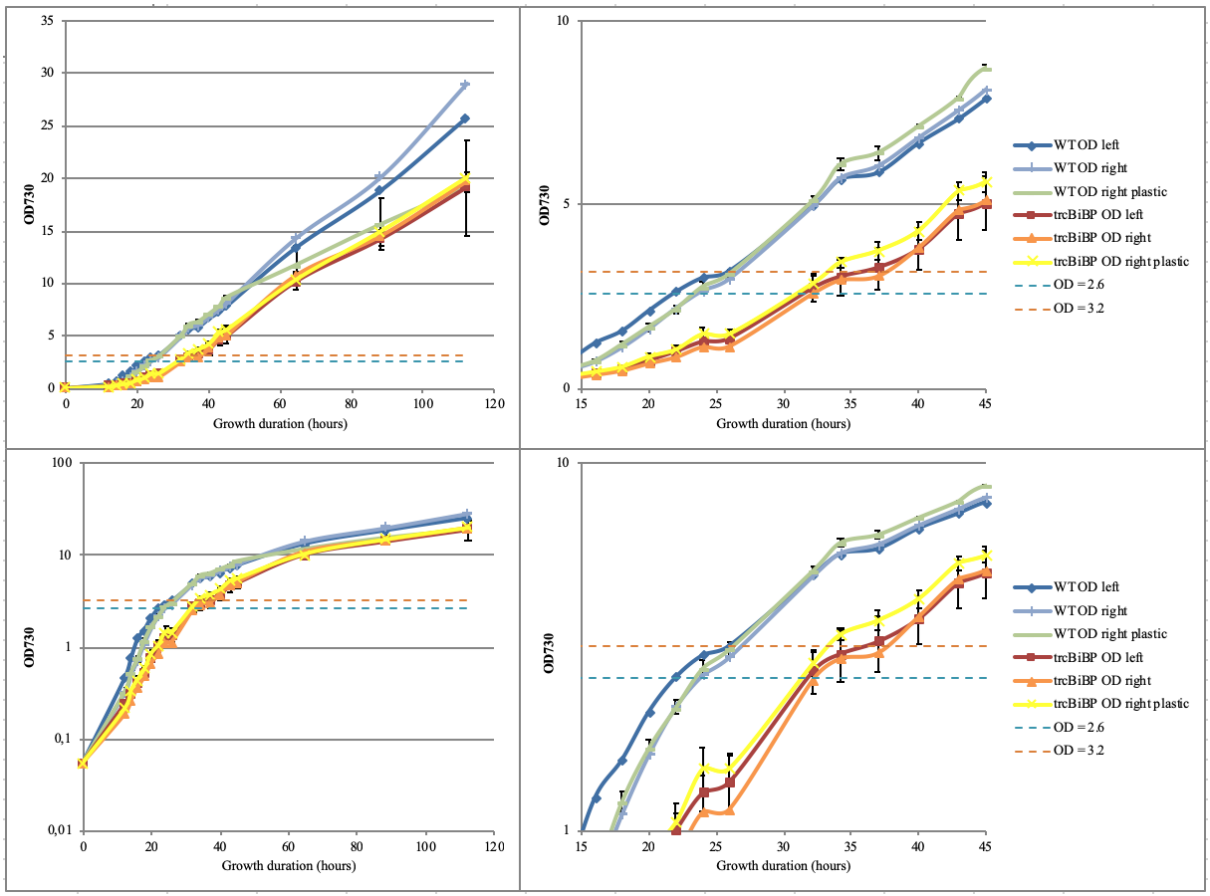

Figure 19: Effect of position in aquarium tank on growth. OD_{730nm} of wild type and trcBiBP over time on three different positions in aquarium: left, right, right with plastic shading. OD_{730nm} displayed on linear (top) and logarithmic scale (bottom). Horizontal axis represents the growth duration in hours. Focused on OD_{730nm} of 1 to 10 (right). wild type OD_{730nm} right plastic, trcBiBP OD_{730nm} left, trcBiBP OD_{730nm} right plastic measured with biological duplicates. Error bars showing the standard deviation of measurements in biological duplicates. wild type OD_{730nm} left, wild type OD_{730nm} right, trcBiBP OD_{730nm} right measured without biological replicates.

Generally, the growth curves of both genotypes showed similar progression despite the different positions in the aquarium tank. Regarding the different positions, in the first 27 hours, wild type showed the fastest growth on the left side of the aquarium which was consistent with the observations of growth in the experiments for carbohydrate characterisation. However, in the last 65 hours of the measurements, wild type grown on the right side showed the fastest growth. TrcBiBP cultures showed slightly faster growth when placed at right side with plastic shading compared to the other two positions. This is inconsistent to previous experiments as trcBiBP cultures grown at the right side obtained a lower OD_{730} than those grown on the left side after 18.5 hours growth duration. OD_{730nm} values over 112 growth hours can be found in Appendix H.

The light intensities on the left, right and right side with plastic shading were 248 ± 38, 186 ± 30 and 208 ± 32 µmol m^{-2} s^{-1}, respectively. The light intensity on the left side was statistically significantly different from the two other positions, right side and the right side with plastic shading ($P < 0.05$; $n = 3$). The shading effect of the plastic seemed to be negligible since the difference between the right side and the right side with plastic shading was not statistically significant ($P > 0.05$; $n = 3$).

3.6 Experiment 3: Effect of initial $NaNO_3$ concentration on growth and glycogen content

Figure 20 depicts the OD_{730nm} (top) of wild type and trcBiBP after 18.5 hours growth in A+ medium with standard nitrogen (N), nitrogen depleted (N-) and nitrogen enriched (N+) conditions. wild type and trcBiBP showed a similar trend with the least growth in normal and the most in nitrogen enriched medium. The difference was more visible in wild type than in trcBiBP. TrcBiBP generally reached lower OD_{730nm} in any of the different nitrogen conditions than wild type after 18.5 hours of growth. The increase of OD_{730nm} of wild type grown in N+ medium compared to N medium was statistically significant ($P < 0.05$; $n = 3$). There was no statistically significant difference of trcBiBP compared to wild type if grown in normal and nitrogen depleted conditions ($P > 0.05$; $n = 3$). In nitrogen enriched conditions, the OD_{730nm} of wild type was significantly different from trcBiBP.

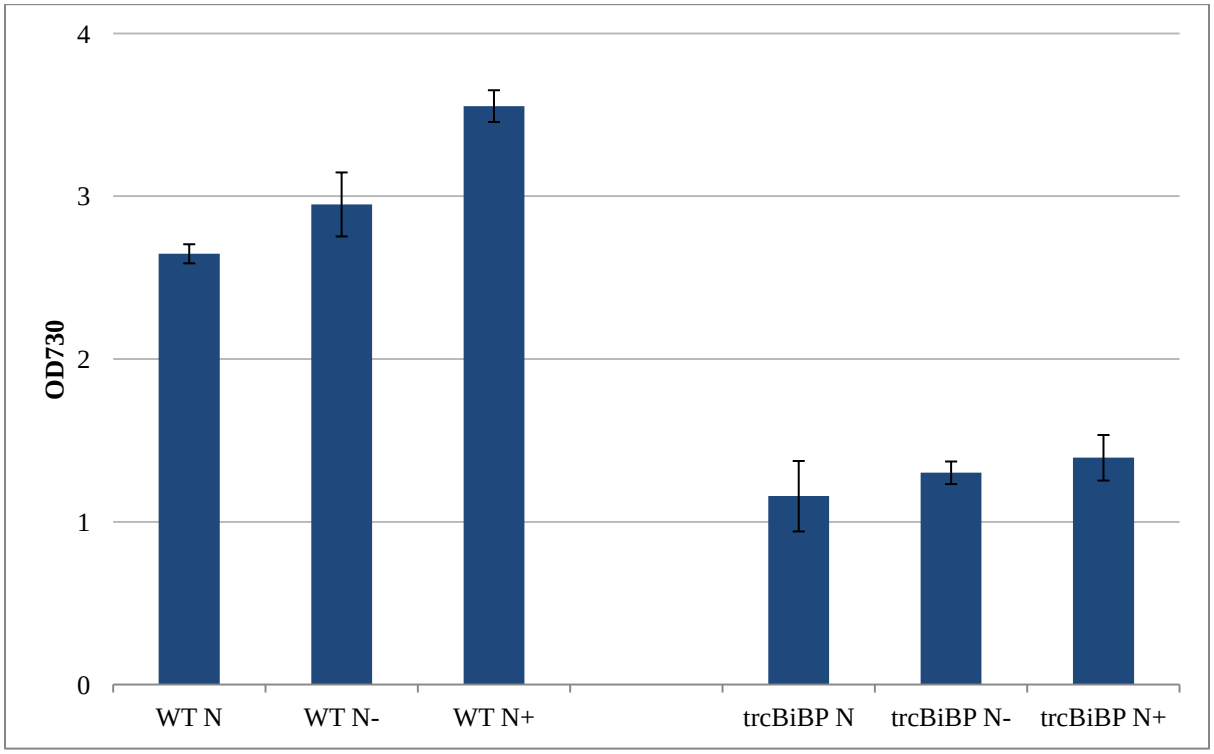

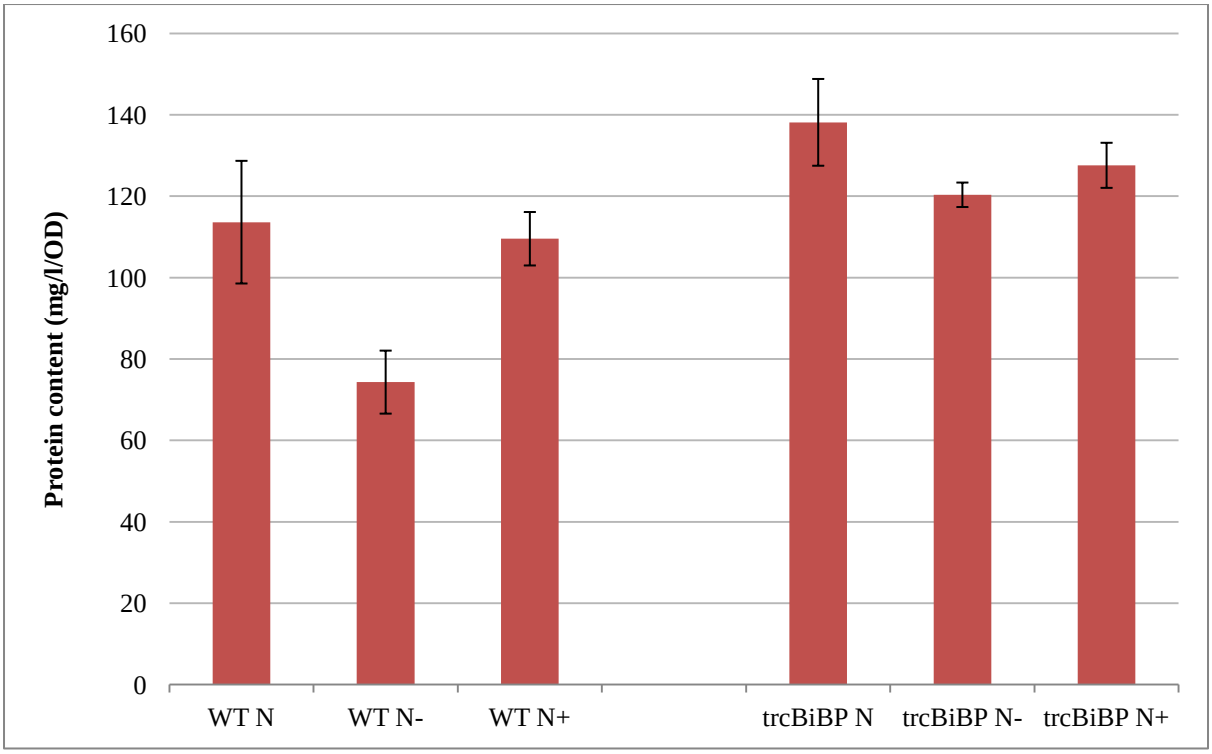

Figure 20: Effect of initial $NaNO_3$ concentration on growth and protein content. OD_{730nm} (top) and protein content (bottom) of wild type and trcBiBP grown for 18.5 hours in A+ medium containing 0.78 g/L (N), 0.28 g/L (N-) and 1.28 g/L (N+) $NaNO_3$, respectively. Error bars show standard deviation of biological duplicates.

Figure 20 (bottom) shows the protein content per OD_{730nm} measured in wild type and trcBiBP after growth in medium with different $NaNO_3$ concentrations. wild type and trcBiBP showed the same trend with the highest protein content after growth in N medium and the lowest protein content when grown in N- medium. The difference in protein content of wild type and trcBiBP grown in N- or N+ medium was not statistically significant compared to growth in N medium ($P > 0.05$; $n = 2$). Comparing the two genotypes to each other, trcBiBP contains more proteins than wild type in all different nitrogen conditions. This is inconsistent with the previous protein measurements where trcBiBP showed lower protein content than wild type when grown in N medium. The specific values for OD and protein content of this experiment can be found in Appendix I.

Figure 21 shows the measured glycogen concentrations in the disrupted pellets of wild type and trcBiBP grown with A+ modified medium with different $NaNO_3$ concentrations. Growth of wild type in N medium resulted in a glycogen concentration of 0.74 mg/L/OD_{730nm} which is consistent with previous experiments that had similar growth conditions. Growth in nitrogen depleted medium increased the glycogen concentration in wild type more than 130 times to 98.36 mg/L/OD_{730nm}. Nitrogen enriched medium caused a 7 fold increase to 5.18 mg/L/OD_{730nm} in wild type compared with N medium. Compared to N, the increased glycogen production of wild type grown with N^- and N^+ medium was statistically significant in a two tail t-test of the logarithmic values ($P < 0.05$; $n = 2$).

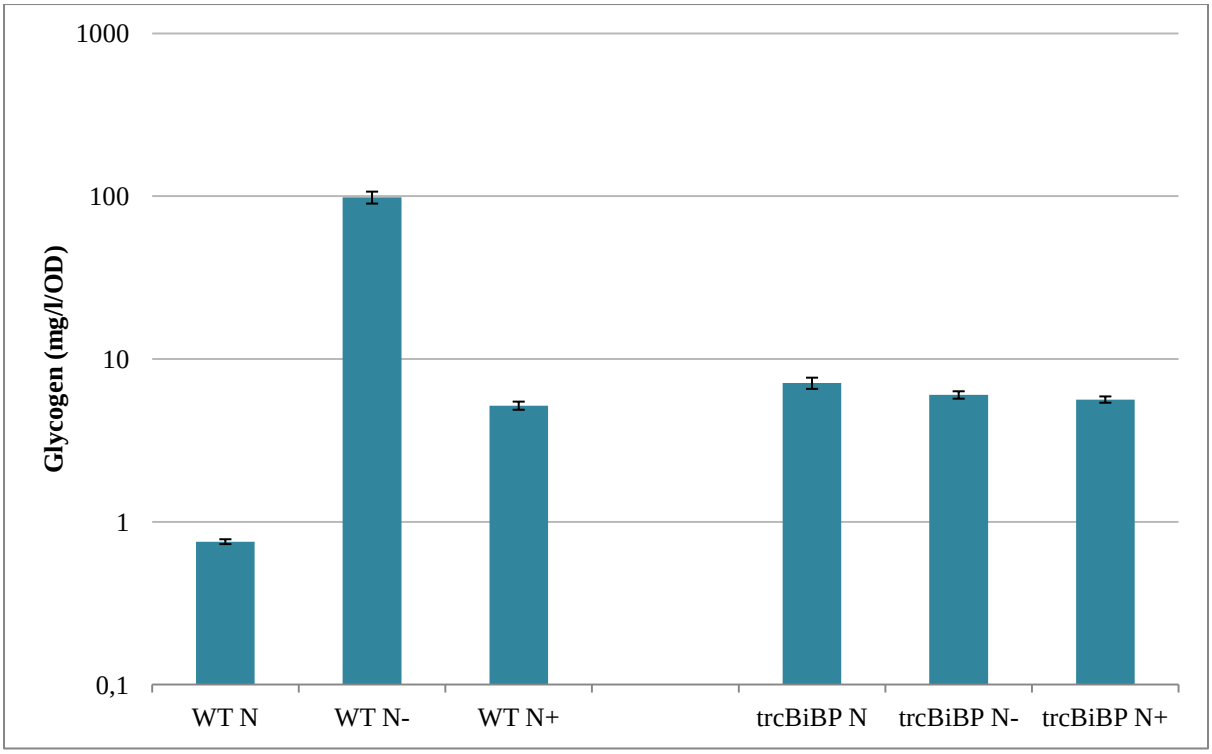

Figure 21: Effect of initial $NaNO_3$ concentration on glycogen. Glycogen concentration in disrupted pellets of wild type and trcBiBP grown in medium with standard nitrogen (N), nitrogen depleted (N-) and nitrogen enriched (N+) medium on a logarithmic scale. wild type and trcBiBP were grown for 18.5 hours in biological duplicates and glycogen digestion and analysis was conducted in technical triplicates. Each value is standardised by dividing by OD_{730nm}. Error bars show standard deviation of biological duplicates.

TrcBiBP showed less differences in the glycogen concentration depending on the $NaNO_3$ concentration in the growth medium than wild type. Glycogen in trcBiBP varied from 5.64 to 7.12 mg/L/OD_{730nm} with the most glycogen detected when grown in N medium and the least in N^+. The measured glycogen concentrations of wild type and trcBiBP grown in N medium were consistent with previous experiments that had similar growth conditions. The differences in glycogen concentration of trcBiBP with N^- or N^+ medium compared to N medium were not statistically significant in a two tail t-test ($P < 0.05$; n = 2). The specific values for glycogen content of this experiment can be found in Appendix I.

4 Discussion

4.1 Growth characterisation and effect of nitrogen

The overexpression of BiBPase was expected to enhance photosynthesis and thereby upregulate the Calvin Benson cycle, resulting in faster growth of trcBiBP compared to wild type. However, contrary to expectations, trcBiBP showed a slower doubling time, resulting in lower OD_{730nm} values per time than wild type (Table 1). This is inconsistent with the previous study where overexpression of BiBPase resulted faster growth due to promotion of CO_2 fixation and repression of respiratory carbon metabolism (De Porcellinis et al., 2018). This inconsistency might be caused by a difference in methodology regarding maintenance of cells and selection of trcBiBP colonies. De Porcellinis et al. (2018) selected larger trcBiBP colonies for the maintenance of the cell lines (Y. Sakuragi, personal communication 28th June, 2019). These colonies were likely larger due to faster growth. In this study,

colonies were selected randomly. Besides, the trcBiBP strain in the study of De Porcellinis et al. (2018) had been maintained on solid medium for more than a year after transformation (Y. Sakuragi, personal communication 28th June, 2019). Since De Porcellinis et al. (2018) used older generations of trcBiBP it seems that the observable effect of the overexpression changes over time. Possibly, the mutation might have initially caused stress in the Synechococcus 7002 cells, resulting in slower growth but the occurrence of secondary mutations mitigated this stress and allowed them to efficiently utilize the upregulation of the Calvin Benson cycle. Alternatively, the effect of the transformation was not identical on all cells, creating a variety of different cells and over time those with an evolutionary advantage such as faster doubling time outcompeted other cells. This could explain the phenotypical differences of the trcBiBP cells obtained by transformation in this study (Figure 9) to those of De Porcellinis et al. (2018). Future quantification of BiBPase activity would be necessary to determine if these differences are caused by a variability in the BiBPase expression.

The transformed cells in this study showed artefacts (Figure 9) and were bigger than the trcBiBP cells from De Porcellinis et al. (2018). According to De Porcellinis et al. (2018) the trcBiBP cell area increased by 36% compared to wild type. In this study, the increase in cell size of trcBiBP amounts yet to 61% (Table 1). Notably, the measured cell sizes of both wild type and trcBiBP are slightly different to the ones reported by De Porcellinis et al. (2018). At least, the cell area of the wild type should coincide but possibly the configurations used in imageJ were different. Therefore, the relative increase of cell area was used as comparison. Apart from the stronger increase in cell size, there appeared to be a yellowish green liquid dispersed close to several trcBiBP cells (Figure 9), suggesting that some of the cells have erupted and died. These observations of artefacts and larger, partially erupted cells were consistent in the repeated transformation.

The discrepancy between the trcBiBP mutant in this study and the previous study of De Porcellinis et al. (2018) can possibly be explained. However, the cause for slower growth of trcBiBP in this study remained unclear. It was hypothesized that trcBiBP was nitrogen starved, resulting in slower growth and accumulation of lipids that were visible as artefacts on the microscopies (Figure 9). Lower biomass production and increased lipid accumulation in nitrogen depleted conditions has been observed in cyanobacteria such as Microcystis panniformis, Microcystis aeruginosa and Microcystis novacekii (Cordeiro et al., 2017) and the microalgae Nannochloropsis oculata and Chlorella vulgaris (Converti et al. (2009)). The cultures in this study were grown in a too low concentration of $NaNO_3$ of 0.78 g/L by mistake as this concentration was stated in the medium preparation protocol (Appendix A). The concentration of $NaNO_3$ in A+ medium is supposed to be 1 g/L (De Porcellinis et al., 2018). 0.78 g/L $NaNO_3$ is referred to as standard nitrogen conditions in this study.

To study the effect of $NaNO_3$, trcBiBP and wild type were grown in standard nitrogen, nitrogen enriched and nitrogen depleted medium. OD_{730nm}, protein content and glycogen content were analysed (Figure 20). Nitrogen enriched conditions resulted in higher ODs of wild type and trcBiBP as nitrogen is important for proteins, ATP and DNA. Nitrogen depleted medium resulted in lower protein content as nitrogen is a crucial element for aminoacid production. TrcBiBP generally showed a higher protein content in the three types of medium compared to wild type. However, this is inconsistent with the results of the growth and carbohydrate characterisation experiment where the protein content of trcBiBP was lower than wild type. Generally, the effect of the altered nitrogen concentration on

growth, protein content and glycogen production of trcBiBP is insignificant, suggesting that nitrogen starvation is not the cause for the slower growth. However, the altered nitrogen conditions had a strong effect on the glycogen production in wild type, resulting in an increase of over 130 times compared to standard conditions (Figure 21). This is consistent with literature studies, observing rapid increase of glycogen content in nitrogen deprived Synechococcus 7002 wild type cells in the first 24 hours of growth. (Jackson et al., 2015) Cyanobacteria like Synechococcus 7002 that are unable to fix nitrogen, accumulate glycogen as a response to nitrogen stress in order to survive. Nitrogen deprivation causes slower growth and reduced demand of building blocks for cellular components and energy for cellular activity, resulting in the storage of excess carbon and energy in form of glycogen. (Shimmori et al., 2018) TrcBiBP did not show this glycogen accumulation, suggesting that the mutation affected its ability to respond to nitrogen stress.

The observations from the Nile Red staining might provide an alternative explanation for the slower growth observed in trcBiBP compared to wild type. The artefacts are likely not lipids because they are fluorescent even without the addition of Nile Red. The autofluorescence rather suggests that the artefacts are pigments (Figure 13). The main pigments found in cyanobacteria are chlorophyl a, four different types of phycobilins and six different carotenoids (Saini et al., 2018). Based on the wavelengths used for excitation (514nm) and maximum peak of emitted light (543nm), the artefacts are most likely phycoerythrins which is one of the four types of phycobilins (Saini et al., 2018). Phycobilins are covalently bound to phycobiliproteins (PBPs) and occur in cyanobacteria cells as phycobilisomes (PBS) containing 300 - 800 assemblies of phycobilins and phycobiliproteins. The diameter of a phycobilisome is around 40 nm (Nobel, 2009) The artefact is significantly larger with a diameter of 703nm, suggesting aggregation of several phycobilisomes. This phenomenon does not seem to be described in literature, at least not as a natural occurrence. However, apparently phycobilisomes aggregate when isolated in a high-salt medium. The fluorescence of those phycobilisomes was quenched due to the aggregation (Glazer et al., 1979). This could indicate that an aggregation of phycobilisomes could result in less efficient light harvesting. Structural changes of the PBS or PBPs could explain the slower growth as “Properly assembled PBPs are important to cyanobacterial light harvesting for growth” (Alvey et al., 2011). However, possible mechanism(s) for a relationship between BiBPase overexpression and aggregation of phycobilisomes remain unclear.

4.2 Saccharides analysis

The disruption efficiencies calculated from the chlorophyll measurements before and after disruption exceeded 100%. It was assumed that in the measurement before disruption, ethanol will extract chlorophyll from the unbroken cells. Furthermore, it was assumed that in the measurement after disruption, there will be no unbroken cells present because those will precipitate in the spinning process. If the latter assumption is not correct, the two measurements are essentially the same. Besides, a disruption efficiency above 100% can be the result of more efficient dissolving of chlorophyll in the measurement after disruption since the cells are already broken, resulting in a higher value than in the measurement before disruption. Intracellular measurements might be underestimated if not all the cells had been disrupted.

According to the methods testing (Figure 14), method 3 appeared to be the most suitable for carbohydrate digestion and analysis because it detected the most accurate concentrations in the

positive controls compared to the other two methods. Therefore, method 3 was used to analyse glucose, glycogen and cellulose in the Synechococcus 7002 strains. Besides, the results from the methods testing indicate that the use of ethanol precipitations leads to lower detection of glucose by the GOPOD assay. It seems that the GOPOD assay detects too low concentration of glucose if this glucose has been dissolved in ethanol and that ethanol was evaporated with the SpeedVac. This effect does not seem to occur as strongly if ethanol was added to precipitate polysaccharides but not to dissolve glucose in it since method 2 showed significantly higher results than method 1. Still, method 2 showed slightly lower results than method 3 where no ethanol precipitations were used. These slightly lower results in method 2 could also be caused by the use of ultrasonication in order to resuspend the ethanol precipitation pellet. The ultrasonication might have released glucose from glycogen which was subsequently subtracted with the glucose and pigment background measurement, resulting in a lower glycogen quantification. All in all, ethanol can potentially be used to remove chlorophylls and precipitate polysaccharides in disrupted Synechococcus 7002 cells but not to dissolve glucose in it as that leads to lower detection by GOPOD after the SpeedVac evaporation step.

The problematics seem to arise particularly in combination with GOPOD assay as ethanol precipitations are widely used in literature for extraction of soluble sugars (Jackson, 2012 and Maness, 2010). A possible explanation for the too low detection of glucose by GOPOD could be that glucose gets degraded or reacts with other compounds in the solution when placed in the SpeedVac. Evaporation of ethanol in the SpeedVac leads to reduction of volume and in that way concentration of the dissolved compounds such as glucose and the medium compounds. Possibly, a compound of the medium bound to glucose molecules and formed a structure that the glucose oxidase can not recognize (/does not fit the active centrum of the glucose oxidase), preventing the production of quinoneimine dye. However, in the DNS assay the SpeedVac is used as well in order to evaporate TFA. In combination with the DNS assay, the use of a SpeedVac does not seem to pose a problem because glucose standards result in the same absorbance values whether they are treated with TFA and placed in a SpeedVac or not. Therefore, degradation of glucose by the SpeedVac is unlikely. If the structure of glucose is altered in the SpeedVac, DNS might still be able to react with it as it is acid and not an enzyme recognizing exclusively one specific physical structure.

If the results of the total sugar estimation are compared to the sum of the results of glycogen, cellulose and glucose, it seems as if all three genotypes consist mainly of other sugars apart from glycogen, cellulose, sucrose and glucose (Figure 17). However, the results from the total sugars assay seem to be less reliable than those from the GOPOD assays because the resuspension after the SpeedVac was not homogeneous due to formation of clumps during the resuspension process. Particles add to the absorbance value, resulting in an overestimation of the measurement. Possibly, this occurrence can be avoided by centrifuging the resuspended samples after the SpeedVac and analysing the supernatant with the DNS assay.

The experiment for growth and carbohydrate analysis of wild type, trcEV and trcBiBP was reproduced and the results of glycogen, cellulose and glucose were similar regarding each biological replicate (Appendix G). The testing of the GOPOD assay by adding known glucose concentrations to medium and to disrupted cells showed similar trendlines (Figure 18). All in all, GOPOD assays appear to be a highly accurate method to quantify glucose-based carbohydrates in *Synechococcus*

PCC 7002 samples. It represents a suitable alternative to HPLC as usage of HPLC in this study resulted in concentrations below the detection range of 100 mg/L.

However, even though the measurement of the carbohydrates with GOPOD seems to be reliable, the specific designation as glycogen and cellulose could be wrong. Depending on the specifications of the glucosidases used, other carbohydrates could be falsely counted as glycogen or cellulose. If there are other carbohydrates with α-D-(1-4) and α-(1,6) glucosidic bonds present, these could be hydrolysed to glucose by amyloglucosidase and lead to an overestimation of glycogen. Similarly, carbohydrates with terminal non-reducing β-D-glucosyl residues could have been converted to glucose by beta-glucosidase and falsely be counted as cellulose. On the other hand, the amount of cellulose is likely underestimated by the amount of cellulose present in crystalline structure. According to literature, more than 60% of the bacterial cellulose is crystalline (Zhao et al., 2015). As described in section 3.4.3, the release of glucose from microcrystalline cellulose with endo-cellulose and beta-glucosidase was barely measurable. Therefore, the cellulose assay likely quantified exclusively amorphous cellulose.

Extracellular carbohydrates could not be detected with DNS or GOPOD assay. Potentially, extracellular carbohydrates are present but in too low concentrations for the DNS or GOPOD assay to detect. In contrast to intracellular carbohydrates that have been concentrated by pelleting the cells, the spent medium has not been concentrated before analysis. Possibly, extracellular carbohydrates could be detected if the spent medium was concentrated for example by lyophilization.

Regarding the glycogen, cellulose and glucose content in the different genotypes, trcBiBP contained more glycogen and cellulose than most of the wild type and trcEV samples (Figure 15). However, the concentrations were measured at just one specific moment in time and might therefore not be representative for the whole genotype if the concentrations are not constant over time. TrcBiBP reached a significantly lower OD than wild type after 18.5 hours and might be in a different growth phase. Therefore, the obtained concentrations might not be comparable as the glycogen content is variable over the growth duration. *Synechococcus* 7002 starts accumulating glycogen when approaching the stationary phase (Jackson et al., 2015). In order to study which growth phase the ODs at 18.5 hours represent, growth curves of wild type and trcBiBP were generated (Figure 19). Based on the obtained growth curves, the cells seemed to enter the stationary phase slowly around an OD_{730nm} of 5. Therefore, the OD_{730nm} values observed after 18.5 hours seem to fall into the exponential growth phase for all genotypes despite the fact that the OD_{730nm} of wild type was almost twice as high as trcBiBP. However, in literature OD_{730nm} values as low as 0.7-1 are designated as late exponential phase (De Porcellinis et al. (2018). In order to obtain holistic, representative values, glycogen and cellulose content should be measured in different stages of each growth phase and the overall outcome compared between the genotypes.

Beside the problematics in comparing glycogen and cellulose of the different genotypes to each other, there is also variability between the different biological replicates visible (Figure 15). There are several factors that might vary among the cultures, potentially leading to different growth conditions. The CO_2 supply might vary due to difference in size of the cotton stopper in the inner tube, porosity and length of the silicon tube connected to the CO_2 tube and distance to the CO_2 source. Furthermore,

the light conditions might be varying depending on the light source used or different light permeability of aquarium tank wall at different positions. Due the gradient in OD_{730nm} and carbohydrate content between the first biological replicate compared to the other two in wild type and trcEV it was hypothesized that the growth conditions on the left and ride side of the aquarium tank were different. The left side seemed to favour more growth and higher glycogen and cellulose production of wild type and trcEV. The higher glycogen and cellulose content could either be caused directly by different growth conditions or indirectly by different growth stages caused by different growth conditions as described above. Even though trcBiBP behaved similar on left and right side, there was slightly higher growth and lower glycogen and cellulose production on the left side. However, due to the rather small difference, it could just be biological variance. The difference in growth of wild type and trcBiBP was studied with OD_{730nm} curves from each side of the aquarium tank (Figure 19). The OD_{730nm} curves confirmed a slightly faster growth on the left side on the aquarium tank of wild type. However, trcBiBP behaved opposite as observed in previous experiments. Besides, both wild type and trcBiBP grew slower than usual, resulting in lower ODs after 18.5 hours than in previous experiments. Some biological replicates did not grow at all initially. This is probably caused by a lag phase due to residues of soap or disinfectant in the tubes which initially inhibited the growth. Therefore, the observed difference in growth at the different positions could also be caused by different initial inhibition.

Likely, the difference in light intensity on the left and the right side, was causing the difference in growth of the biological replicates. To test this possibility, the light sources could be swapped in order to study if the different growth and carbohydrate productions consequently occur on opposite sides.

Despite the variability of growth conditions, trcBiBP generally seemed to contain more glycogen than wild type which is opposite to the outcome of the previous study (Figure 15). According to De Porcellinis et al. (2018), trcBiBP contained lower glycogen than wild type, likely due to repression of ADP-glucose pyrophosphorylase, an important enzyme for glycogen synthesis, by an increased amount of inorganic phosphate from the overexpression of BiBPase. This discrepancy might be caused by difference between the trcBiBP cells in the two studies. As mentioned before, the trcBiBP cells in this study appeared larger and contained artefacts, potentially aggregated phycobilisomes, and slower growth than the trcBiBP cells from De Porcellinis et al. (2018). The cause for different growth might as well affect the carbohydrate composition. Besides, the methodology regarding carbohydrate analysis was different in the study in De Porcellinis et al. (2018). *Synechococcus* 7002 cells were grown at 1g/L $NaNO_3$ and harvested in the exponential phase (De Porcellinis et al., 2018), accordingly at an OD_{730nm} of below 1. Potentially, other growth parameters such as light intensity and CO_2 might differ as well, as they are not quantified in this study. This difference in growth conditions might affect the behaviour of trcBiBP directly. Additionally, the circumstance that wild type showed variable results due to varying growth conditions in the carbohydrate analysis might reduce its reliability when functioning as reference (Figure 15).

Identifying the influencing factor(s) that caused the differences, can not only be useful in order to eliminate it to ensure constant growth conditions for representative results but also to gain insight into factors that affect growth and carbohydrate production of wild type and trcBiBP. Besides, since carbohydrates are not the only carbon-based building blocks, total carbon should be quantified by

using an elemental analyzer in order to determine to what extent the overexpression of BiBPase leads to increased carbon fixation.

4.3 Evaluation of wild type or trcBiBP to produce feedstock for biorefineries

The objective of this project was to analyse the carbohydrate composition of *Synechococcus* 7002 wild type and trcBiBP in order to evaluate their usability for glucose production as feedstock in biorefineries. Initially, trcBiBP seemed to be the more promising candidate. According to previous studies, trcBiBP showed faster growth, increased extracellular production of soluble sugars compared to wild type (De Porcelinis et al., 2018). Using extracellular sugars as feedstock for heterotrophic organisms, has the advantage that it requires less processing steps than using intracellular carbohydrates. Intracellular carbohydrates require processing steps such as cell disruption and enzymatic hydrolysis of polysaccharides. However, the trcBiBP strain obtained with tri-parental conjugation showed opposite characteristics than those described by De Porcelinis et al. (2018). Identifying the cause for the observed differences of trcBiBP according to De Porcellinis et al. (2018) and this study could lead to improvement of the obtained trcBiBP strain and increase its potential for producing carbohydrates as a feedstock.

According to the results of this study, wild type grown in nitrogen depleted medium seems to be the most suitable option for feedstock production due to the rapid increase of glycogen content (Figure 21). Besides, another study demonstrated the successful fermentation to ethanol by *Saccharomyces cerevisiae* (Möllers et al., 2014). Based on the results of this study, the productivity of wild type in nitrogen depleted conditions is around 0.38 kg glucose/m^3/day. Under the same conditions, the productivity of trcBiBP is only around 0.010 kg glucose/m^3/day. In comparison, the productivity of corn crop is 0.0025 kg/m^2/day, assuming yield, glucose content and growth duration to be 5 tons corn per hectare, 61% and 4 months, respectively (Quintero et al., 2008). However, a direct comparison of the productivities of *Synechococcus* 7002 and corn crops proves difficult due to difference in dimensional units. Besides, more factors than the productivity alone are determining for economic feasibility as photobioreactors are expensive to operate (Mobin et al., 2014).

5 Conclusions

The objective of this project was to study the effect of overexpressing BiBPase on the carbohydrate production of the cyanobacterium *Synechococcus* 7002 in order to evaluate its potential as feedstock producer for biorefineries. According to the results of this study, overexpression of BiBpase caused increased cell size, slower growth, aggregation of phycobilisomes and increased cellulose and glycogen content. However, the growth conditions in the experimental setup were varying, leading to variability in the biological replicates. For instance, the increase in glycogen content was not statistically significant due to the variability of the wild type replicates.

Growth and carbohydrate distribution observed in trcBiBP was contradictory with a previous study. De Porcellinis et al., (2018) reported faster growth, decreased glycogen content and increased extracellular carbohydrates of trcBiBP compared to wild type. Since De Porcellinis et al. (2018) used

older generations of trcBiBP it seems that the observable effect of the overexpression changed over time either due to secondary mutations or outcompetition of slower growing cells.

Nitrogen deprivation was found to barely affect growth and glycogen production of trcBiBP, eliminating this as a cause for the slower growth. However, consistently with literature studies (Möllers et al., 2014) nitrogen deprivation lead to accumulation in *Synechococcus* 7002 wild type. Nitrogen depleted medium lead to 130 times increase of glycogen content in wild type compared to standard nitrogen conditions. This results in a productivity of 0.38 $kg/m^3/day$, making it a promising candidate to produce carbohydrates for biorefineries.

Future research is required for further optimisation of carbohydrate production with *Synechococcus* 7002. As mentioned before, characterisation of the carbohydrate composition at different stages of the growth would result in a more representative analysis of each genotype. Besides, further optimisation of trcBiBP could potentially lead to creation of a mutant with an even higher productivity than wild type. If the trait of faster growth observed in trcBiBP of De Porcellinis et al. (2018) can be combined with glycogen accumulation from nitrogen depleted medium and excretion as extracellular monosaccharides. This mutant would represent an ideal candidate for production of feedstock for biorefineries, increasing the probability of economic application.

6 Acknowledgements

We would like to express our gratitude to our supervisors Dr. Yumiko Sakuragi, Dr. Cristiano Varrone and Dr. Mette Lübeck, for their patient guidance, encouragement and valuable and constructive suggestions on this research. We would also like to thank Dr. Panagiotis Lymperopoulos and Dr. Maria Rasmussen for their advice and assistance in the laboratory. As well as the department of Plant and Environmental Sciences of Copenhagen University and the section of Sustainable Biotechnology of Aalborg University for providing the resources to perform this research.

We would also like to extend our thanks to all our teachers and colleagues from the master program in Sustainable Biotechnology from Aalborg University, Copenhagen for their support and feedback during the development of this thesis.

7 Bibliography

Alvey, R. M., Biswas, A., Schluchter, W. M., & Bryant, D. A. (2011). Effects of modified phycobilin biosynthesis in the cyanobacterium Synechococcus sp. strain PCC 7002. *Journal of bacteriology*, *193*(7), 1663-1671.

Batterton, J. C., & Van Baalen, C. (1971). Growth responses of blue-green algae to sodium chloride concentration. *Archiv für Mikrobiologie*, *76*(2), 151-165.

Converti, A., Casazza, A. A., Ortiz, E. Y., Perego, P., & Del Borghi, M. (2009). Effect of temperature and nitrogen concentration on the growth and lipid content of Nannochloropsis oculata and Chlorella vulgaris for biodiesel production. *Chemical Engineering and Processing: Process Intensification*, *48*(6), 1146-1151.

Cordeiro, R. S., Vaz, I. C., Magalhaes, S., & Barbosa, F. A. (2017). Effects of nutritional conditions on lipid production by cyanobacteria. *Anais da Academia Brasileira de Ciências*, *89*(3), 2021-2031.

Cotton, C. A., Kabasakal, B. V., Miah, N. A., & Murray, J. W. (2015). Structure of the dual-function fructose-1, 6/sedoheptulose-1, 7-bisphosphatase from Thermosynechococcus elongatus bound with sedoheptulose-7-phosphate. *Acta Crystallographica Section F: Structural Biology Communications*, *71*(10), 1341-1345.

De Porcellinis, A. J., Nørgaard, H., Brey, L. M. F., Erstad, S. M., Jones, P. R., Heazlewood, J. L., & Sakuragi, Y. (2018). Overexpression of bifunctional fructose-1, 6-bisphosphatase/sedoheptulose-1, 7-bisphosphatase leads to enhanced photosynthesis and global reprogramming of carbon metabolism in Synechococcus sp. PCC 7002. *Metabolic engineering*, *47*, 170-183.

Glazer, A. N., Williams, R. C., Yamanaka, G., & Schachman, H. K. (1979). Characterization of cyanobacterial phycobilisomes in zwitterionic detergents. *Proceedings of the National Academy of Sciences*, *76*(12), 6162-6166.

Höök, M., & Tang, X. (2013). Depletion of fossil fuels and anthropogenic climate change—A review. *Energy Policy*, *52*, 797-809.

Jackson, P., & Gallagher, J. T. (Eds.). (2012). *A laboratory guide to glycoconjugate analysis*. Birkhäuser.

Jackson, S. A., Eaton-Rye, J. J., Bryant, D. A., Posewitz, M. C., & Davies, F. K. (2015). Dynamics of photosynthesis in a glycogen-deficient glgC mutant of Synechococcus sp. strain PCC 7002. *Appl. Environ. Microbiol.*, *81*(18), 6210-6222.

Kamm, B., & Kamm, M. (2004). Principles of biorefineries. *Applied microbiology and biotechnology*, *64*(2), 137-145.

Kingsley, G. R. (1939). The determination of serum total protein, albumin, and globulin by the biuret reaction. Journal of biological chemistry, 131, 197-200.

Maness, N. (2010). Extraction and analysis of soluble carbohydrates. In *Plant stress tolerance* (pp. 341-370). Humana Press.

Markley, A. L., Begemann, M. B., Clarke, R. E., Gordon, G. C., & Pfleger, B. F. (2014). Synthetic biology toolbox for controlling gene expression in the cyanobacterium Synechococcus sp. strain PCC 7002. *ACS synthetic biology*, *4*(5), 595-603.

Mobin, S., & Alam, F. (2014, December). Biofuel production from algae utilizing wastewater. In *19th Australasian Fluid Mechanics Conference* (pp. 1-7).

Möllers, K. B., Cannella, D., Jørgensen, H., & Frigaard, N. U. (2014). Cyanobacterial biomass as carbohydrate and nutrient feedstock for bioethanol production by yeast fermentation. *Biotechnology for biofuels*, *7*(1), 64.

Nobel, P. S. (2009). Chapter 5 - Photochemistry of Photosynthesis, In P. S. Nobel (Ed.) *Physicochemical and Environmental Plant Physiology (Fourth Edition)* (pp. 228-275). Academic Press

Quintero, J. A., Montoya, M. I., Sánchez, O. J., Giraldo, O. H., & Cardona, C. A. (2008). Fuel ethanol production from sugarcane and corn: comparative analysis for a Colombian case. *Energy*, *33*(3), 385-399.

Rumin, J., Bonnefond, H., Saint-Jean, B., Rouxel, C., Sciandra, A., Bernard, O., ... & Bougaran, G. (2015). The use of fluorescent Nile red and BODIPY for lipid measurement in microalgae. *Biotechnology for biofuels*, *8*(1), 42.

Saini, D. K., Pabbi, S., & Shukla, P. (2018). Cyanobacterial pigments: Perspectives and biotechnological approaches. *Food and chemical toxicology*, *120*, 616-624.

Sanchez, O. J., & Cardona, C. A. (2008). Trends in biotechnological production of fuel ethanol from different feedstocks. *Bioresource technology*, *99*(13), 5270-5295.

Shimmori, Y., Kanesaki, Y., Nozawa, M., Yoshikawa, H., & Ehira, S. (2018). Transcriptional Activation of Glycogen Catabolism and the Oxidative Pentose Phosphate Pathway by NrrA Facilitates Cell Survival Under Nitrogen Starvation in the Cyanobacterium Synechococcus sp. Strain PCC 7002. *Plant and Cell Physiology*, *59*(6), 1225-1233.

Zhao, C., Li, Z., Li, T., Zhang, Y., Bryant, D. A., & Zhao, J. (2015). High-yield production of extracellular type-I cellulose by the cyanobacterium Synechococcus sp. PCC 7002. *Cell Discovery*, *1*, 15004.

8 Appendix

Appendix A: Chemical composition of A+ medium per liter.
[1] As explained in section 4.1, the $NaNO_3$ concentration in A+ medium is supposed to be 1.0 g/l. In experiment 3, the $NaNO_3$ concentration was adapted to 0.28 g/l (nitrogen depleted medium (N-)) and 1.28 g/l (nitrogen enriched medium (N+)).

Chemical	**Weight per litter**
$MgSO_4 \cdot 7H_2O$	5.0 g
NaCl	18 g
KCl	0.6 g
$NaNO_3$	0.78 g[1]
$CaCl_2 \cdot 2H_2O$	0.37 g
Na_2EDTA	30 mg
KH2PO4	50 mg
$FeCl_3 \cdot 6H_2O$	3.89 mg
Tris	1 g
H_3BO_3	34.3 mg
$MnCl_2 \cdot 4H_2O$	4.32 mg
$ZnCl_2$	0.315 mg
Na2MoO4.2H2O	0.03 mg
CuCl2	0.003 mg
$CoSO4.7H_2O$	0.01215 mg

Appendix B: Schematic summary of experiment 1. Colonies were transferred from solid to liquid medium for pre-cultures. Pre-cultures were used as inoculum for cultures. After growth, a culture samples was taken for OD_{730} measurement, cell count, cell size analysis and Nile Red staining. One drop of the culture was transferred to solid medium and the colonies were used as PCR template. The rest of the culture was centrifuged. The supernatant was analysed for extracellular carbohydrates with GOPOD and DNS assay. The cell pellets are disrupted and analysed for proteins with BCA assay and intracellular carbohydrates with GOPOD and DNS.

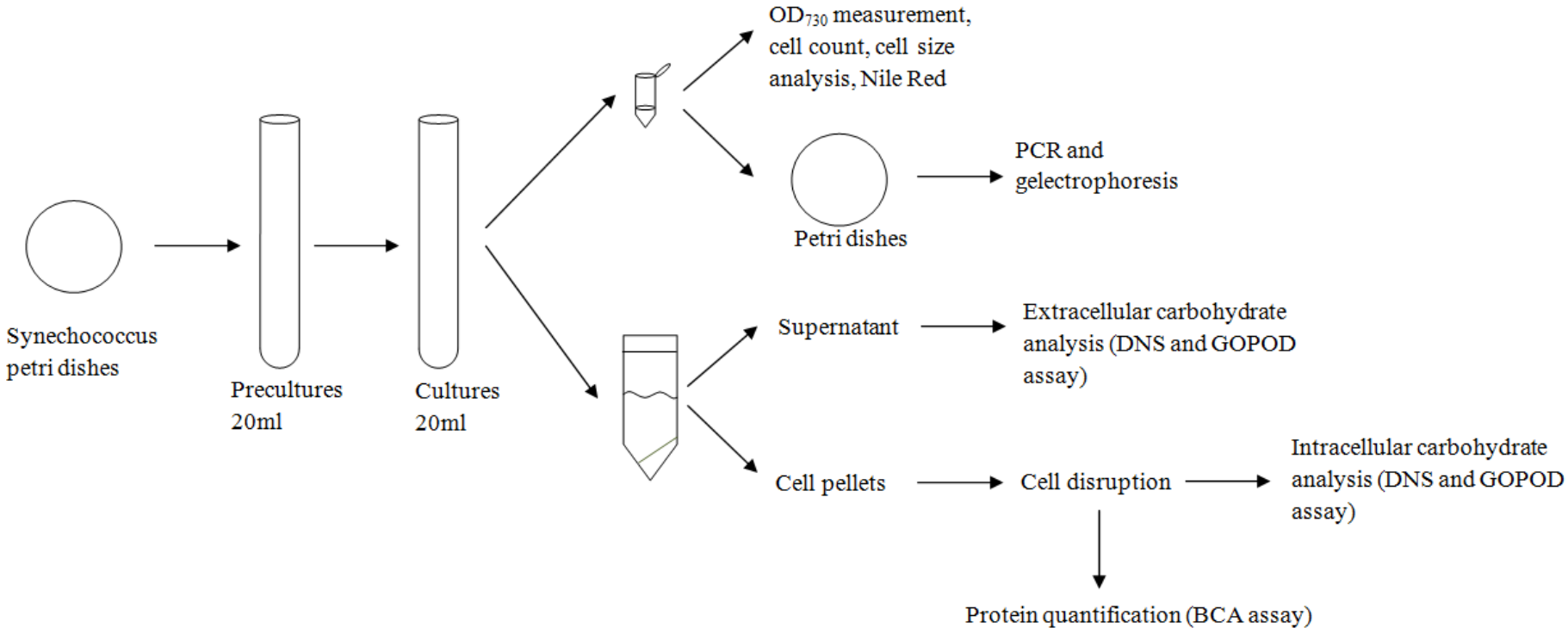

Appendix C: Schematic summary of experiment 2. Colonies were transferred from solid to liquid medium for pre-cultures. Pre-cultures were used as inoculum for cultures. After growth, a culture samples was taken for OD_{730} measurement, cell count, cell size analysis and Nile Red staining. One drop of the culture was transferred to solid medium and the colonies were used as PCR template. The rest of the culture was centrifuged. The supernatant was analysed for extracellular carbohydrates with GOPOD and DNS assay. The cell pellets are disrupted and analysed for proteins with BCA assay and intracellular carbohydrates with GOPOD and DNS.

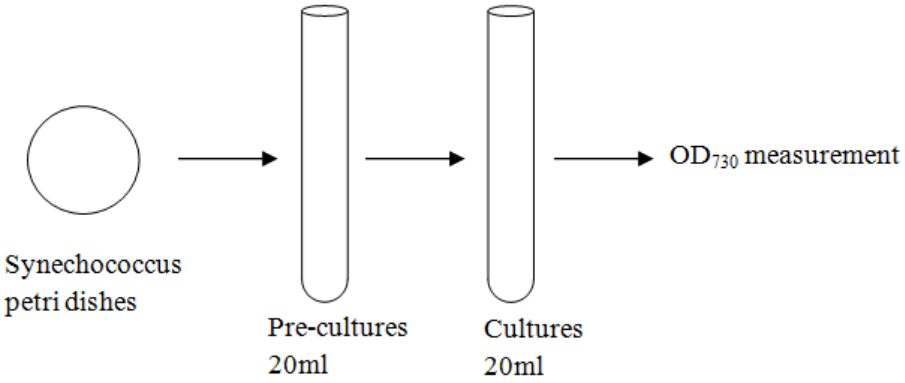

Appendix D: Schematic summary of experiment 3. Colonies were transferred from solid to liquid medium for pre-cultures. Pre-cultures were used as inoculum for cultures. During growth, culture samples were taken for OD_{730} measurement. The rest of the culture was centrifuged. The cell pellets are disrupted and analysed for proteins with BCA assay and intracellular glycogen with GOPOD assay.

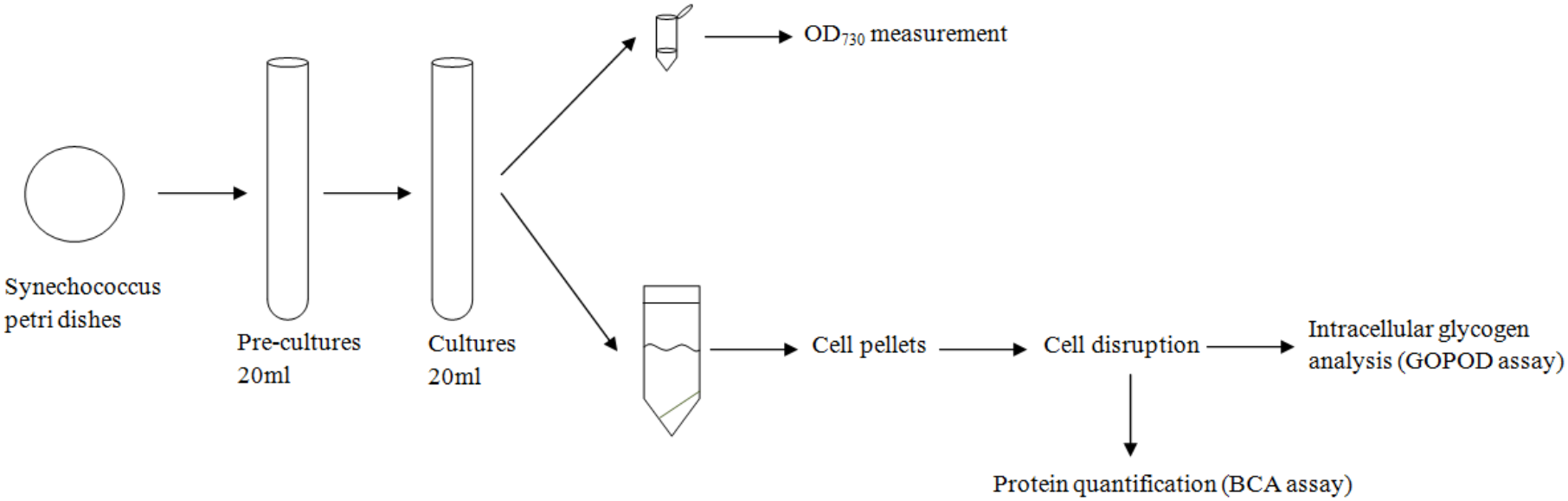

Appendix E: Analysis of glucose released from digested glycogen from one sample per genotype (WT. EV. NB). one negative control (C-) and five positive controls (C+1 to C+7) with three different methods. Method 1: three ethanol precipitations. method 2: one ethanol precipitation. method 3: no ethanol precipitations. Error bars showing the standard deviation of the technical duplicates.

	Method 1	**Method 2**	**Method 3**
Unit	*mg/l glycogen*	*mg/l glycogen*	*mg/l glycogen*
WT	0.66	0.88	1.72
trcEV	0.58	1.74	1.78
trcBiBP	0.64	3.07	3.39
C-	0.11	0.19	0.17
C+1 (0.5 mg/l)	0.16	0.22	0.31
C+2 (2.5 mg/L)	0.23	0.72	1.41
C+3 (5 mg/l)	1.21	1.67	2.79
C+4 (10 mg/l)	1.08	3.97	5.60
C+5 (15 mg/l)	1.73	6.75	7.30

Appendix F: Growth and saccharide content of biological replicates of Synechococcus wild type. trcEV and trcBiBP. OD, cell count, cell size, protein, glucose, sucrose, glycogen, cellulose and total sugars content is displayed, as well as p values resulting from the statistical analysis. P values above 0.05 are coloured orange, p values below 0.05 are coloured blue. Not applicable values denoted (N.A.), as well as values below the sensitivity (b.S.)

[2] not standardized by OD

[3] one tailed t-test used for statistical analysis

Measurement	**OD**	**Cell count**	**Cell area**	**Protein content**	**Glucose**	**Sucrose**	**Glycogen**	**Cellulose**	**Total reducing sugars**
Unit		*10^7 cells/ml/OD*	*μm^2*	*mg/L/OD*	*mg/L/OD*	*mg/L/OD*	*mg/L/OD*	*mg/L/OD*	*mg/L/OD*
WT1	3.38	11.64	N.A.	139.60	1.00	b. S.	6.00	3.37	15.14
WT2	2.62	9.40	N.A.	138.38	b. S.	b. S.	0.80	0.72	8.36
WT3	2.84	7.94	N.A.	131.46	b. S.	b. S.	0.81	0.88	11.19
trcEV1	2.23	8.22	N.A.	160.33	0.47	b. S.	2.17	1.73	12.34
trcEV2	1.86	7.61	N.A.	149.68	b. S.	b. S.	0.75	0.76	9.15
trcEV3	2.08	5.33	N.A.	112.78	b. S.	b. S.	0.67	0.77	8.88
trcBiBP1	1.60	5.86	N.A.	124.02	b. S.	b. S.	3.92	2.42	11.45
trcBiBP2	1.40	7.25	N.A.	154.18	b. S.	b. S.	4.74	3.00	12.98
trcBiBP3	1.28	6.57	N.A.	109.49	b. S.	b. S.	4.98	3.18	13.72
C-[2]	b. S.	b. S.	N.A.	b. S.	b. S.	b. S.	b. S.	b. S.	b. S.
Mean WT	2.95 ±0.39	9.66 ±1.86	3.52 ±0.9	136.48 ±4.39	1.00	N.A.	2.54 ±3.00	1.66 ±1.48	11.56 ±3.40
Mean trcEV	2.06 ±0.18	7.05 ±1.52	4.13 ±2.2	140.93 ±24.95	0.47	N.A.	1.20 ±0.84	1.09 ±0.56	10.12 ±1.92
Mean trcBiBP	1.43 ±0.16	6.65 ±0.70	5.66 ±0.9	129.23 ±22.80	N. A.	N.A.	4.54 ±0.56	2.87 ±0.39	12.72 ±1.16
p for H0: WT=trcBiBP	0.01	0.04[3]	2.40E-38	0.64	N.A.	N.A.	0.37	0.29	0.62
p for H0: WT=trcEV	0.04	0.07[3]	4.35E-08	0.79	N.A.	N.A.	0.52	0.58	0.57
p for H0: trcBiBP=trcEV	0.01	0.32[3]	3.19E-23	0.58	N.A.	N.A.	0.01	0.01	0.13

Appendix G: Repetition of intracellular carbohydrates analysis; glucose, glycogen and cellulose concentration of the biological triplicates of wild type, EV, trcBiBP and C- obtained with GOPOD assay. The error bars show the standard deviation of the technical triplicates. Each value was standardised by dividing by OD except for C-.

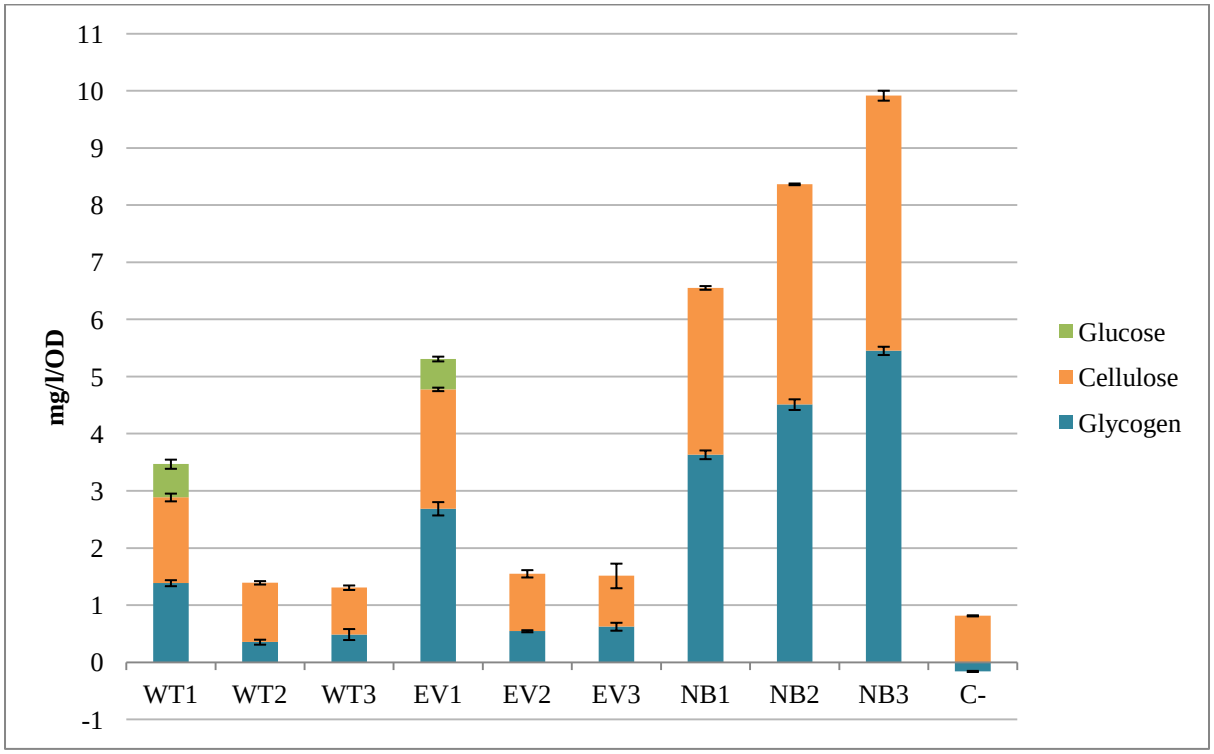

Appendix H: OD_{730nm} values of WT and *trcBiBP* at three different positions in the aquarium tank (left, right, right with plastic shading) over a duration of 112 growth hours. Doubling time and corresponding P value from statistical analysis are shown. Not applicable values denoted (N.A.).

OD730																		**Doubling time**
Growth duration (hours)	**0**	**12**	**14**	**16**	**18**	**20**	**22**	**24**	**26**	**32**	**34**	**37**	**40**	**45**	**64**	**88**	**112**	**h^{-1}**
WT OD left average	0.06	0.47	0.77	1.24	1.57	2.12	2.63	3.01	3.20	4.99	5.69	5.87	6.67	7.87	13.40	18.85	25.73	2.48
WT OD right average	0.06	0.32	0.50	0.72	1.11	1.62	2.18	2.66	2.99	4.97	5.72	6.05	6.82	8.13	14.30	20.14	28.98	2.76
WT OD right plastic average	0.06	0.33	0.54	0.76	1.20	1.68	2.17	2.78	3.13	5.13	6.10	6.41	7.13	8.72	11.77	15.64	19.12	2.58
trcBiBP OD left average	0.06	0.25	0.31	0.42	0.55	0.77	1.01	1.28	1.37	2.74	3.04	3.29	3.79	5.05	10.23	14.29	19.18	4.85
trcBiBP OD right average	0.06	0.19	0.26	0.36	0.48	0.67	0.85	1.13	1.15	2.59	2.94	3.05	3.82	5.13	10.83	14.62	19.80	4.17
trcBiBP OD right plastic average	0.06	0.22	0.34	0.45	0.59	0.86	1.06	1.48	1.49	2.87	3.43	3.75	4.29	5.64	10.39	15.01	20.11	3.99
WT mean	0.06	0.37	0.60	0.90	1.29	1.81	2.32	2.82	3.11	5.03	5.84	6.11	6.87	8.24	13.16	18.21	24.61	2.61±0.14
trcBiBP mean	0.06	0.22	0.31	0.41	0.54	0.77	0.97	1.29	1.34	2.73	3.14	3.36	3.97	5.27	10.48	14.64	19.70	4.43±0.45
P value for H0: WT=trcBiBP	N.A.	N.A.	N.A.	N.A.	N.A.	N.A.	N.A.	N.A.	N.A.	N.A.	N.A.	N.A.	N.A.	N.A.	N.A.	N.A.	N.A.	0.02

Appendix I: OD, protein content and glycogen content of Synechococcus wild type and trcBiBP grown with N, N- and N+ medium. P values resulting from the statistical analysis are shown. P values above 0.05 are coloured orange, p values below 0.05 are coloured blue.
[2] not standardized by OD
[4] statistical analysis conducted with logarithmic values

Measurement	**OD**	**Protein content**	**Glycogen**		Statistical analysis			
Unit		*mg/L/OD*	*mg/L/OD*					
WT N 1	2.73	134.92	0.72		Mean WT N	2.65 ±0.12	113.62 ±30.13	0.76 ±0.05
WT N 2	2.56	92.31	0.79		Mean WT N-	2.95 ±0.39	74.32 ±15.47	98.36 ±16.58
WT N- 1	2.67	85.26	86.64		Mean W N+	3.55 ±0.20	109.55 ±13.14	5.18 ±0.60
WT N- 2	3.23	63.38	110.09					
WT N+ 1	3.69	118.84	4.75		Mean trcBiBP N	1.16 ±0.43	138.14 ±21.32	7.12 ±1.13
WT N+ 2	3.42	100.26	5.60		Mean trcBiBP N-	1.3 ±0.14	120.34 ±6.01	6.02 ±0.63
trcBiBP N 1	0.85	123.07	7.91		Mean trcBiBP N+	1.39 ±0.28	127.58 ±11.08	5.64 ±0.50
trcBiBP N 2	1.46	153.22	6.32					
trcBiBP N- 1	1.20	116.09	6.47		p for H0: WT N = WT N-	0.46	0.28	0.01[4]
trcBiBP N- 2	1.40	124.60	5.58		p for H0: WT N = WT N+	0.05	0.88	0.01[4]
trcBiBP N+ 1	1.20	119.75	5.99		p for H0: WT N- = WT N+	0.24	0.14	0.00[4]
trcBiBP N+ 2	1.59	135.42	5.28					
C- N[2]	0.00	-40.02	-11.50		p for H0: trcBiBP N = trcBiBP N-	0.72	0.44	0.36
C- N-[2]	0.00	438.75	-11.91		p for H0: trcBiBP N = trcBiBP N+	0.59	0.62	0.25
C- N+[2]	0.00	-40.86	-10.18		p for H0: trcBiBP N- = trcBiBP N+	0.73	0.52	0.58